
This is the **accepted version** of the journal article:

Schoch, Rainer R.; Seegis, Dieter; Mujal, Eudald. «The Middle Triassic vertebrate deposits of Kupferzell (Germany) : Palaeoenvironmental evolution of complex ecosystems». *Palaeogeography, Palaeoclimatology, Palaeoecology*, Vol. 603 (October 2022), art. 111181. DOI 10.1016/j.palaeo.2022.111181

This version is available at <https://ddd.uab.cat/record/264843>

under the terms of the  license

1 **The Middle Triassic vertebrate deposits of Kupferzell (Germany):**
2 **palaeoenvironmental evolution of complex ecosystems**

3

4 Rainer R. Schoch^{1,2}, Dieter Seegis¹, Eudald Mujal^{1,3,*}

5

6 ¹Staatliches Museum für Naturkunde Stuttgart, Rosenstein 1, D-70191 Stuttgart, Germany

7 ²Universität Hohenheim, Fachgebiet Paläontologie, Institut für Biologie, D-70599 Stuttgart,
8 Germany

9 ³Institut Català de Paleontologia Miquel Crusafont, ICTA-ICP building, c/ de les columnes,
10 s/n, E-08193 Cerdanyola del Vallès, Catalonia, Spain

11

12 *Corresponding author: eudald.mujalgrane@smns-bw.de

13

14 **Abstract**

15 In 1977, within three months of excavation, a 500 m spanning road-cut near Kupferzell
16 (southern Germany) produced a total of ~30,000 vertebrate remains from the Middle
17 Triassic Lower Keuper. The bulk of the material stems from two temnospondyl
18 amphibians, *Gerrothorax pulcherrimus* (~70%) and *Mastodonsaurus giganteus* (~30%),
19 with the pseudosuchian archosaur *Batrachotomus kupferzellensis* ranging first among
20 the other remains. Analyses of data collected during excavation, supplemented by new
21 fieldwork, provide rich information on the sedimentary setting as well as the
22 development of the fauna and their ecosystems. The sequence consists of: basal coaly
23 mudstones (K1), massive siltstones (K2), green siliciclastic mudstones (K3), yellow to
24 pale brown marlstones (K4), and yellow massive dolostones (K5). The deposits
25 comprise a succession of similar water bodies that were emplaced on a lacustrine to
26 floodplain setting in which carbonate muds dominated. Two main lake systems, with
27 intermittent/periodical marine influence, as well as relatively stark periods of
28 drought, harboured complex vertebrate ecosystems. These were dominated by a
29 relatively high diversity of fishes and temnospondyl amphibians with a lesser, but
30 notable, presence of archosaurs, forming the top predators of the trophic web. The
31 sequence records alternating periods of flooding and desiccation, shaping a relatively
32 complex environmental setting that was likely prone to the presence of life, eventually

33 becoming an exceptional fossil lagerstätte. Kupferzell, together with nearby
34 contemporaneous localities, represent relatively diverse and complex ecosystems
35 (including several top predators) that allow understanding the evolution and
36 palaeoecology of Middle Triassic vertebrate communities, including the groups that
37 diversified during the Mesozoic era.

38

39 **Key words**

40 Keuper, sedimentology, taphonomy, fossil lagerstätte, lacustrine,
41 palaeoenvironmental evolution

42

43 **1. Introduction**

44

45 Middle Triassic vertebrate communities may form the key to our understanding
46 of how modern biotic communities evolved. In recent years, our knowledge of the
47 early stages of the Mesozoic has notably increased, especially because of a better
48 understanding and sampling of localities of Early Triassic age (Romano et al., 2020).
49 However, the terrestrial fossil record from the earliest part of the Triassic is still
50 incomplete. An impoverishment of ecosystems has been hypothesised on the basis of
51 harsh environmental conditions after the Permian–Triassic biotic crisis (Chen and
52 Benton, 2012; Sun et al., 2012, Irmis and Whiteside, 2012). However, the magnitude of
53 this mass extinction on land remains still unresolved and questioned (see Lucas, 2017,
54 2021 for discussion). The Middle Triassic fossil record is notably richer than that of the
55 Early Triassic, showing that the so-called modern tetrapod groups already radiated
56 were dominant in the ecosystems, with lepidosauromorphs, archosauriforms and
57 pseudosuchians experiencing major diversifications, while temnospondyl amphibians
58 were still abundant (e.g., Sues and Fraser, 2010; Schoch and Seegis, 2016).
59 Nevertheless, even if the Middle Triassic ecosystems are better known than those of
60 the Early Triassic, the temporal and geographic origin and/or diversification of some
61 groups (which by the Late Triassic were globally distributed) remain still unclear. In
62 order to overcome this lack of knowledge and potential biases in fossil preservation,
63 integrative studies combining stratigraphical, sedimentological and palaeontological

64 analyses (i.e., leading to the identification of taphonomic pathways and
65 palaeoecological features) are basic.

66 In this regard, the mixed terrestrial-shallow marine Lower Keuper facies from
67 southwestern Germany are particularly informative for the understanding of Middle
68 Triassic continental ecosystems and the identification of potential biases in the
69 preservation of vertebrates. In this region, a range of fossil lagerstätten are known for
70 their abundance of fossils and quality of preservation (Wild, 1980; Hagdorn et al., 2015;
71 Schoch and Seegis, 2016; Schoch et al., 2018; Mujal and Schoch, 2020; Mujal et al., 2022).
72 Among these, the Kupferzell locality was the first to be discovered and also yielded
73 the largest quantity of vertebrate fossils collected in a single period. This locality was
74 exploited in an emergency excavation during the construction of a highway in spring,
75 1977 and yielded a total of ~30,000 bones including numerous excellently preserved
76 skulls and partial skeletons (Wild, 1978a, 1978b, 1979, 1980).

77 In this work, we describe and analyse in detail the stratigraphic and
78 sedimentary framework of this locality that was first briefly characterised by Urlichs
79 (1982). We focus on elucidating the palaeoenvironmental evolution of these rich and
80 diverse vertebrate deposits. Despite a large number of publications dealing with the
81 tetrapod fauna at Kupferzell (Gower, 1999; Schoch, 1999; Hellrung, 2003; Gower and
82 Schoch, 2009; Schoch and Sues, 2014; Hagdorn et al., 2015; Schoch et al., 2018; Hinz et
83 al., 2020; Mujal et al., 2022), no comprehensive sedimentological and detailed
84 taphonomic analyses were hitherto available.

85 Here we intend to fill this gap by focusing on the rich data of this important
86 fossil vertebrate lagerstätte. The objectives of the present work are to (1) describe the
87 sedimentary and taphonomic features of the Kupferzell locality, (2) reconstruct the
88 depositional history of the fossiliferous beds, and (3) compare the findings with those
89 on the coeval and equally rich locality at Vellberg-Eschenau (Schoch and Seegis, 2016).
90 The present work aims to contribute to a deeper understanding of the Middle Triassic
91 terrestrial (lacustrine)-coastal ecosystems and their significance at the dawn of the
92 Mesozoic.

93

94 **2. Geological setting**

95

96 The Kupferzell excavation site encompassed a 500 m long E-W strip along the
97 federal highway (Autobahn) A6, located between Heilbronn and Nürnberg in
98 southern Germany (Fig. 1). The fossiliferous horizons were exposed only during the
99 road works, which lasted from March to the first days of June, 1977 (Wild, 1978a,
100 1978b). The Lower Keuper (Lettenkeuper, Erfurt Formation; Middle Triassic, late
101 Ladinian, Longobardian) crops out over vast areas of the Hohenlohe plain in northern
102 Württemberg (Fig. 1A). In the region of the Kupferzell (north) and Untermünkheim
103 (south) municipalities, the upper part of the Erfurt Formation is regularly exposed in
104 road cuts and during house building (Fig. 1B).

105 The succession was deposited in the Central European Basin (CEB; Eetzold and
106 Schweizer, 2005), which had intermittent connections to the Tethys Sea during the
107 Triassic. In the study area, the 20–25 m spanning Lower Keuper (Erfurt Formation)
108 overlies the 50–100 m thick Upper Muschelkalk (Warburg Formation; late Anisian–
109 early Ladinian), a massive carbonate unit that formed in a shallow epicontinental sea
110 (e.g., Franz et al., 2013, 2015; Hagdorn et al., 2021). The subsequent deposition of the
111 Lower Keuper (late Ladinian) occurred within the framework of a restricted
112 connection of the CEB with the Tethys (Pöppelreiter and Aigner, 2003, 2008). In N-NE
113 direction, the succession is composed of more terrigenous deposits, whereas towards
114 S-SW (including the study area) the unit consists of a mixed, alternating carbonate-
115 siliciclastic succession (Fig. 1A) on an epicontinental platform (Brunner and Bruder,
116 1977; Brunner, 1980; Pöppelreiter and Aigner, 2003, 2008; Beutler et al., 1999; Franz et
117 al., 2013; Nitsch, 2015). The Lower Keuper is overlain by the Middle Keuper (Grabfeld
118 Formation; Carnian), which contains thick deposits of gypsum and fine-grained
119 reddish siliciclastic deposits (e.g., Franz et al., 2014). Thus, from the Upper
120 Muschelkalk to the Middle Keuper, transgressive-regressive sequences are recorded
121 (Pöppelreiter and Aigner, 2003, 2008; Franz et al., 2013), and the Lower Keuper
122 generally represents a transition from marine to terrestrial environments.

123

124 **3. Methods**

125

126 The first vertebrate fossils were found by the private collector Johann Wegele
127 who informed Rupert Wild (Staatliches Museum für Naturkunde Stuttgart, SMNS),

128 who then set up a large-scale excavation in the course of the construction of the federal
129 highway A6. The fossils were collected during the salvage campaign from March 14 to
130 June 3, 1977 by a crew of the SMNS, supported by a number of volunteers, including
131 engaged private collectors. All the recovered fossils stem from the Untere Graue
132 Mergel (UGM, Lower Grey Marls) unit within the upper half of the Lower Keuper
133 (Figs. 1A, 2). After removing the overlying, hard dolostone bed (the Anoplophora-
134 Dolomite unit) with hydraulic shovels, the fossiliferous marlstones and mudstones
135 were dug off by hand using picks and scrapers, and the vertebrate fossils were
136 recovered using standard palaeontological procedures, including both mechanical and
137 acid preparation (Wild, 1978a, 1978b, 1979). A total of 1000 m² were excavated.
138 Preparation was carried out in the course of the following years at the SMNS lab
139 facilities. Many of these fossils have now been prepared, but a large number of
140 “common” specimens still awaits preparation, mostly single bones of *Gerrothorax* and
141 *Mastodonsaurus*. Great quantities of fossiliferous marlstones and mudstones were
142 screen-washed in the laboratory for microfossils, and the residues were hand-picked
143 and sorted by a range of volunteers over 20 years. As many microvertebrate remains
144 contain diagenetically generated cracks, screen washing usually produces more or less
145 fragmented remains.

146 A second, smaller outcrop of the Lower Keuper was accessible for a short time
147 in July 1983, about 1200 m east of the Kupferzell Autobahn (highway) site. Here, a
148 trench for a gas pipeline was excavated, exposing yellow-brown marlstones rich in fish
149 remains, probably correlating with the upper, yellow-brown unit K4 (see sections 4
150 and 6 below) at the Kupferzell site. This site is informally known as “Gasleitung
151 Kupferzell” (Fig. 1B). Screen washing and subsequent picking of the residues from this
152 site produced many well-preserved microvertebrate remains, mostly of fishes, but also
153 including numerous tiny tetrapod bones and teeth.

154 At the excavation site, stratigraphic sections encompassing the whole
155 outcropping portions of the Lower Keuper were measured by Urlichs (1982). Herein,
156 these sections are reviewed and updated (Fig. 2). In the present work, we have
157 extensively reviewed the available sedimentological samples, including large blocks
158 embedding still unprepared fossils that allowed us to examine sedimentological
159 features and reconstruct the stratigraphic succession of the most fossiliferous layers in

160 the main excavation sites (North- and South-side in Figs. 1B, 2). In order to provide a
161 context of the Kupferzell lagerstätte within the Lower Keuper, we mainly follow the
162 methods of Schoch and Seegis (2016). In the present work, each unit (a total of five) is
163 identified by a number, running from base to top, and preceded with a “K” (referring
164 to Kupferzell) (see also nomenclature of the layers for stratigraphically equivalent
165 localities in Schoch and Seegis, 2016). This nomenclature has been correlated with the
166 previous descriptions by Wild (1980) and Urlichs (1982), as well as with unpublished
167 notes taken during the excavation.

168 In order to complement the facies descriptions, we have carried out a
169 microfacies analysis by examining thin sections under a petrographic microscope
170 Leica DM750P, with a camera Leica ICC50 W incorporated to photograph the samples
171 (using the software LAS EZ v.3.4.0). Thin sections have been prepared at the SMNS lab
172 facilities for the present study, following standard procedures for their production,
173 with a thickness of ~25–30 µm. The thin sections include all the layers of the lagerstätte
174 units (K3, K4) from different areas of the excavated site, as well as from the underlying
175 unit (K2).

176 With the reconstruction of the stratigraphic profile in detail (layer by layer),
177 including also lateral changes, the succession of facies and microfacies has been
178 restored. Similarly, the distribution and relative abundance of lithological
179 components, tetrapod remains and other fossils within the stratigraphic succession
180 have been elucidated (Figs. 3, 4). In some cases, the layers in which bones were
181 recovered were annotated during the excavations. In the cases where this was not
182 done, we have examined the matrix remains around and within the bones, as well as
183 the colour of the bones, and compared these features with those from which the layer
184 was already known, allowing us to precisely (re-) locate the fossils within the
185 stratigraphic succession.

186 The tetrapod bones from Kupferzell stored in the SMNS collections, as well as
187 some from the Muschelkalkmuseum (MHI, Ingelfingen) were examined in detail in
188 order to identify taphonomic features. We have primarily followed the methods and
189 classification by Behrensmeyer (1978) and Haynes (1983) for the preservation stages
190 and fractures of bones, respectively. Further references are included in the
191 corresponding descriptions and interpretations.

192 Regarding the estimated proportions of the different taxa, the context in which
193 the excavation took place, under much pressure due to the road construction, has to
194 be considered. Approximately, remains of *Gerrothorax* represent around 70% of the
195 finds, with those of *Mastodonsaurus* being somewhat less than 30%, while all other taxa
196 are proportionally much less frequent (Wild, 1980). It is of course difficult to decide in
197 retrospect how to count such amounts. Firstly, around only a quarter of all finds have
198 been prepared and secondly, prior to the preparation, specific research was focused
199 on skulls, mandibles and shoulder girdle bones, while smaller and postcranial
200 elements had lower priority and are still awaiting preparation. Therefore, a recording
201 of the prepared pieces may only reproduce a potentially biased image. In addition, it
202 is also possible that smaller bones were not collected in the appropriate frequency
203 during the excavation because the team was under enormous time pressure. It was
204 inevitable that the careful recovery of the valuable skulls was in the foreground, and
205 last but not least, surrounding bones may be sacrificed when large blocks protected by
206 plaster jackets are prepared for extraction, which is inevitable even with the most
207 modern excavation techniques. Overall, however, even after recounting the prepared
208 and unprepared finds for *Gerrothorax* and *Mastodonsaurus*, a ratio of 2:1 is confirmed.
209 It is surprising how rare other tetrapods and vertebrates are, because the ratio is
210 different at all other well-known sites, as further discussed in the present work.

211

212 **4. Stratigraphy, sedimentary facies and fossil content**

213

214 The fossil-rich (mass accumulation) sequence is restricted to the upper part of
215 the Untere Graue Mergel (UGM), immediately below the base of the Anoplophora-
216 Dolomite (Figs. 1–4), forming the focus of the present work. This stratigraphic position
217 has produced similar fossil lagerstätten in various localities within a range of 30 km,
218 such as Kupferzell-Bauersbach, Vellberg-Eschenau, Ummenhofen, Ilshofen,
219 Wolpertshausen and Crailsheim-Neidenfels (Urlichs, 1982; Hagdorn et al., 2015;
220 Schoch and Seegis, 2016; Schoch et al., 2018).

221 The fossiliferous sequence from the upper portion of the UGM at Kupferzell
222 was first described by Wild (1978a, 1978b, 1979, 1980) and Urlichs (1982). Here we
223 provide a new and detailed description for all the units (each composed by either one

224 or multiple layers, see below) within the uppermost UGM succession together with
225 new palaeoenvironmental interpretations. The features (e.g., thickness, lithology,
226 colouration, sedimentary structures, and fossil contents) of each layer are mainly based
227 on those from the main excavation sites (North- and South-sides in Figs. 1, 2), although
228 they are further complemented with information from other sections nearby.
229 Interestingly, some of these units present lateral facies changes (Urlichs, 1982), which
230 are discussed in section 6 below.

231 The analysed sequence includes the following units, from base to top: (1) dark
232 coaly mudstones with green mudstones in the top (K1: 70 cm); (2) brown to greenish-
233 grey siltstones with red nodules (K2: 10–20 cm); (3) green mudstones with an erosive
234 base and abundant mud cracks (K3: 10–25 cm); (4) yellow marlstones with erosive base
235 (K4a: 5–10 cm) followed by light brown marlstones with calcitic crusts (K4b: 5–15 cm)
236 and yellow marlstones with carbonate fossiliferous concretions (K4c: 20 cm); (5)
237 massive yellow dolostone (K5: 20 cm). Units K1 to K4 correspond to the top of the
238 UGM, whereas unit K5 forms the base of the Anoplophora-Dolomite (Figs. 2, 3). Units
239 K3 and K4 constitute the main portion of the fossil lagerstätte (Figs. 3, 4).

240

241 *4.1. Dark coal-bearing and green mudstones (K1: 70 cm)*

242

243 The stratigraphic sequence of the Kupferzell fossil lagerstätte starts with a
244 black-grey, coal-bearing clayey mudstones that contains small, broken bones, fish
245 scales and teeth (Urlichs, 1982). The Lower Keuper coals have been identified as
246 lignites (Nitsch, 2015). Coal seams embedded in mudstones and siltstones are known
247 from many Lower Keuper localities of northern Württemberg (southern Germany) and
248 are mostly found in the upper third of the UGM (Schoch and Seegis, 2016), but also in
249 the Sandige Pflanzenschiefer, the unit of the underlying sequence (Quenstedt, 1880;
250 Brunner, 1973, 1977; Urlichs, 1982; Weber, 1992; Pöppelreiter, 1999; Hagdorn et al.,
251 2015; EM and RRS pers. obs.). In the vicinity of the Kupferzell excavation site, a thick
252 coal-bearing mudstone unit was reported by Urlichs (1982) both west and east of the
253 excavation area, being poorly exposed in the excavation site itself (Fig. 2). The lignite
254 in the Lower Keuper originated either from autochthonous hygrophilic plants, as
255 evidenced by horizons with abundant fossil roots (rhizcretions), or from plant

256 material that was washed in from the mainland and the shore region. In the latter case,
257 the coal would thus be formed by the accumulation of allochthonous material.
258 Conceivably, the short-term ingression of a shallow sea in the Kupferzell area might
259 have prompted the presence of hygrophilic plants, while the hinterland was
260 significantly drier (Nitsch, 2015). This is suggested by spores and pollen from such
261 plant groups (Urlichs, 1982). Rivers and smaller streams probably transported plant
262 remains into lagoons and restricted/protected areas at the sea shore. Elsewhere in
263 these carbonaceous layers there are skulls and skeletal remains of mastodonsaurids,
264 trematosaurids and plagiosaurids (e.g., in the Gaildorf locality, see Hagdorn et al.,
265 2015), suggesting that these temnospondyl amphibians did not live far away from
266 these settings. At Herdtlingshagen, 3 km east of the Kupferzell site (Figs. 1B, 2), Urlichs
267 (1982) found a rich bivalve fauna (*Bakevellia*, *Myophoria*, *Unionites*) and brachiopods
268 (*Coenothyris*) within the lateral equivalent of K1, accompanied by characeans, fish
269 scales, and temnospondyl bones. The identified bivalves and brachiopods indicate a
270 marine to brackish water settings (see Geyer et al., 2005), whereas characeans indicate
271 more freshwater conditions (Urlichs, 1982). Therefore, as a whole, the unit K1
272 represents a mixture of environments, suggesting frequent transgression-regression
273 episodes on the sea level.

274

275 4.2. Brown siltstones (K2: 10–20 cm)

276

277 The coal-bearing unit K1 is followed by 10–20 cm thick, hard, brown to
278 greenish-grey siltstones. They contain dark red stains, reddish ironstone nodules, iron-
279 impregnated root tubules, and horizontally orientated claystone flasers. This unit (K2)
280 has been observed in a radius of at least 2.5 km. The siltstones are highly resistant to
281 weathering and therefore much easier to find in fields than the unconsolidated
282 mudstones and marlstones that embed them.

283 The thin section of this unit shows that the siltstones are mostly composed of
284 small-sized sub-rounded to rounded quartz grains, all of them having similar size (Fig.
285 5A-C). The matrix is composed of claystones, mostly formed by tiny (often
286 unidentifiable) minerals. Some phyllosilicate crystals of micaceous minerals (likely
287 muscovite) with a size similar to that of the quartz grains are present. Quartz grains

288 (maximum size ~0.1 mm) represent around 40% of the components, whereas large
289 mica crystals represent around 5%, or even less. The greenish colouration is given by
290 subangular, equidimensional green clasts of chlorite that represent 5-10% of the
291 components. No gradation or preferential orientation of any component is observed
292 within the thin section. A distinctive feature is the presence of reddish opaque halos
293 (Fig. 5A-C), generally oval-shaped and horizontally elongated, though sometimes they
294 display irregular shapes and/or are arranged in multiple elongated bands parallel to
295 each other. These reddish structures include quartz grains, which are notably less
296 abundant than within the reddish halos. The oval-shaped halos may form concentric
297 rings, with bands being less reddish in-between darker ones (Fig. 5A). The borders of
298 the halos are either sharp or diffuse. The thickest rings display less quartz grains and
299 are more opaque. Given the concentric, oval shape of most of these reddish structures,
300 they most probably form pedogenetic nodules of ferric composition; i.e., representing
301 the ironstone nodules mentioned by Urlichs (1982). During their growth they absorbed
302 the quartz grains, explaining the reduction in abundance of this silicate.

303 The siltstones contain the bivalve *Myophoria transversa*, which tolerated normal
304 saline waters (Geyer et al., 2005), suggesting that the unit K2 is of marine or lagoonal
305 origin. In addition, its top contains sedimentary structures formed by rapid water
306 flows (Wild, 1980). At the excavation site, the siltstones had an undulating upper
307 surface (Wild, 1980; Urlichs, 1982; Fig. 2), suggesting erosional processes after its
308 deposition, with elongated channels identified in some areas. Such gullies are evidence
309 of channels or rapid water flows. Presumably, those were fluvial channels likely
310 generated in the initial phases of a marine regression. As a whole, these siltstones
311 represent the topmost part of a sequence with increasingly more shallow marine
312 deposits that was eventually covered by sediments originated in freshwater
313 conditions. In fact, the uneven relief on top of the siltstones is filled up by the green
314 mudstones of the unit K3 (Urlichs, 1982; Fig. 2). On the other hand, non-marine
315 influence during formation of K2 is indicated by the presence of the ostracod
316 *Darwinula*, a genus that nowadays lives in freshwater or very weak brackish
317 environments (Hagdorn et al., 2015). The siltstones of the unit K2 were present in
318 outcrops to the west and southwest of the excavation, but absent towards the east (Fig.
319 2). At Wolpertshausen (12 km east of the Kupferzell site), a coquina with coaly flakes,

320 mass accumulations of bivalves (*Bakevella*, *Myophoria* and *Pleuromya* at the base,
321 *Unionites* in the top), has been reported by Urlich (1982) and Hagdorn et al. (2015) in
322 the stratigraphic level of unit K2.

323 In summary, this unit highlights the marine influence in the area, although it
324 also testifies a regression trend, especially because of the increasing influence of the
325 shore region and the settlement of freshwater settings as indicated by the overlying
326 unit K3, as well as the presence of ferruginous nodules, further suggesting seasonally
327 drained substrates (e.g., Tabor et al., 2008).

328

329 4.3. Green mudstones (K3: 10–25 cm)

330

331 The siltstones of the unit K2 are overlain by an unconsolidated, green mudstone
332 sequence in which bones, teeth and fish scales are accumulated. This unit spans some
333 1.5 km E-W (Urlich, 1982; RRS and DS pers. obs.). It forms the basal part of the
334 Kupferzell fossil lagerstätte *sensu stricto*. In the periphery of the lagerstätte, it forms a
335 rather undifferentiated olive-green mudstone sequence, whereas at the main
336 excavation area two types of facies can be distinguished (Fig. 6).

337 In the excavated area, unit K3 contained large quantities of vertebrate fossils.
338 Most finds consist of isolated bones that are well preserved and somewhat darker
339 brown than those found in unit K4. Fishes are mostly represented by scales, sometimes
340 accumulated in clusters, but never as articulated skeletons. The tetrapod finds include
341 more than 10 complete skulls of *Mastodonsaurus giganteus* (Jaeger, 1828) that are
342 excellently preserved but mostly somewhat flattened by compaction. They were all
343 embedded with the dorsal side up, with one exception, which forms an unusually
344 three-dimensionally preserved specimen (Schoch, 1999). In addition, at least one giant
345 skeleton of *Mastodonsaurus* was found (SMNS 81310), covered by a calcareous crust,
346 near the top of unit K3 (Wild, 1980), as well as hundreds of single bones from all parts
347 of the skeleton, some of which containing bite traces (Mujal et al., 2022). The bulk of
348 the material is formed by isolated elements of the plagiosaurid *Gerrothorax*
349 *pulcherrimus* (Hellrung, 2003), which also includes a few disarticulated skeletons of
350 that taxon. Notably, even skull elements of *Gerrothorax* were accumulated as single

351 bones in large quantities, indicating that there was sufficient time for the skulls to
352 decay, despite their firm suturing.

353 Much rarer are single bones of the temnospondyls *Kupferzellia wildi* Schoch,
354 1997, *Plagiosuchus pustuliferus* (Fraas, 1896) and *Trematolestes hagdorni* Schoch, 2006,
355 and the chroniosuchian *Bystrowiella schumanni* Witzmann et al., 2008, each of these
356 represented by a few elements only (0.05% of the total hypodigm). Only few single
357 bones of small amniotes were found among the microvertebrate remains, of which
358 small vertebrae of a choristodere-like diapsid (Schoch, 2015) form the only identifiable
359 taxon at present. Scores of tetrapod teeth were also found, mostly from *Mastodonsaurus*
360 and smaller temnospondyls, accompanied by teeth of *Batrachotomus kupferzellensis*
361 Gower, 1999 and a putatively fish-eating archosaur similar to, but not identical with
362 *Jaxtasuchus salomoni* Schoch and Sues, 2014 (see tooth type R5 of Schoch et al., 2018).
363 Notably, *Jaxtasuchus* itself and other reptiles common at Vellberg-Eschenau are absent.

364 Several disarticulated skeletons (4–5) of *Batrachotomus* were found on top of unit
365 K3, with the upper surface of the bones reaching into the topping layer K4a (Wild,
366 1980). The yellow, marly sediment of layer K4a can still be seen inside tooth alveoli
367 and unprepared parts of bones. These skeletons were apparently deposited after the
368 formation of K3 and must have remained on the dry surface for a longer time.

369 The green mudstones are rich in fish remains, which include scales, bones and
370 teeth from 14 fish taxa: the elasmobranchs *Acrodus* cf. *lateralis* Agassiz, 1839, *Hybodus*
371 aff. *keuperianus* (Winkler, 1880), and *Lissodus subhercynicus* Dorka, 2001, the
372 actinopterygians *Saurichthys* sp., a *Gyrolepis*-like palaeonisciform, an indeterminate
373 actinopterygian with perleidid-like dentition, "*Thelodus*" *inflexus* Schmid, 1861,
374 *Dipteronotus* sp., *Serrolepis suevicus* Dames, 1888, a redfieldiiform, a scanilepiform, an
375 actinistian, a new medium-sized dipnoan (formerly identified as "*Ferganoceratodus*
376 *concinus*" [Plieninger, 1842]), and the large dipnoan *Ptychoceratodus serratus* (Agassiz,
377 1838) (see Schultze, 1981). Even though several of these taxa were evidently
378 euryhaline, this whole association is typical for freshwater to oligohaline beds in the
379 Lower Keuper (Böttcher, 2015; see also discussion in Pawlak et al., 2022).

380 Many tetrapod bones were accumulated in the channel-like depressions on top
381 of unit K2 (Urlichs, 1982). Freshwater ostracods (*Darwinula liassica* [Brodie, 1843]) are
382 much more abundant than euryhaline ostracods (*Pulviella teres* [Seebach, 1857],

383 *Speluncella elegans* Beutler and Gründel, 1963). The units K3 and K4 contain remains of
384 characean algae, whose reproductive organs (oogonia) were deposited in large
385 quantities.

386 Below we describe the two main types of deposits that form unit K3 (Fig. 6).
387 They show remarkable differences in composition (with a micritic or siliciclastic
388 matrix) as well as structure (massive or laminated). Of note, the facies type with non-
389 carbonate matrix and massive aspect (Figs. 5D, 6A-G; section 4.3.1 below) is more
390 common than the type with carbonate matrix and laminated/layered (Fig. 6H-J;
391 section 4.3.2 below). Because the excavation had to proceed under heavy time
392 pressure, detailed stratigraphic and sedimentological data could not be collected,
393 therefore, it is not possible to unravel with confidence the spatial distribution of these
394 two types of facies. The collected blocks encompassing the whole unit K3 show that
395 such unit is either the massive mudstones or the laminated mudstones, and no
396 combination or gradation from one facies to the other has been observed. Therefore, it
397 appears that the laminated mudstones (less abundant than the massive one) were
398 localised in specific areas. The two facies types also present similarities, the most
399 remarkable being the presence of green clasts (chlorite) that give the characteristic
400 green coloration to the unit K3 (Fig. 6).

401

402 4.3.1. *Massive non-carbonate green mudstones*

403 This facies is composed of relatively soft, pale green mudstones (Figs. 5D, E,
404 6A). Their grain size and microscopic composition (Fig. 6B-G) characterizes them as
405 fine, clayey siltstones, though the base is slightly coarser, being even very fine-grained
406 sandstones at some parts (Fig. 6F, G). These deposits were observed infilling the
407 depressions on top of the underlying massive siltstones (K2). This facies of unit K3 has
408 a massive aspect (Figs. 5D, E, 6A) and is pale olive green in fresh condition and light
409 green in the dry state. It splits into cm-thick units that have light brown or beige stains
410 on the (rough) bedding plane (Fig. 7A, B). Occasionally, there appear oval-shaped
411 fragments composed of claystones (i.e., finer-grained) that may correspond to clay
412 chips (Fig. 6A, B). A distinctive feature of this massive mudstone facies is the presence
413 of mud cracks (Fig. 7), described in detail in section 4.3.3 below.

414 These deposits contain numerous clay flakes of various colours, ranging from
415 pale grey to intense green and light blue, as well as tiny muscovite flakes, the latter
416 being well-visible in the thin sections (Fig. 6B-G). The clayey siltstones of K3 are poor
417 in fossil remains. Fish scales and teeth (light brown) occur regularly only within the
418 mud cracks, which belong the unit K4 (see section 4.3.3 below). When a piece of K3 is
419 submerged in water, it decays into green, sterile clay clasts and the coarser fossiliferous
420 matrix K4. A clear-cut lamination is absent in this facies of unit K3, but muscovite
421 flakes and other clasts are loosely arranged in layers.

422 Thin sections of this facies of unit K3 (Fig. 6B-G) reveal a similar lithological
423 composition to that of unit K2, but mineralogical proportions are notably different.
424 Quartz grains in are sub-rounded to rounded as in unit K2, but they are generally
425 much less abundant (around 10-15% of the components) and smaller than in unit K2;
426 thus the claystone matrix predominates (Fig. 6B-E). Nevertheless, in localised small
427 portions of the layer, and especially from the base of the unit K3 (Fig. 6F, G), quartz
428 grains are slightly larger and more abundant (~20%), but in any case not as much as
429 in the siltstones of the unit K2. Muscovite crystals (as revealed by their pale coloration
430 and transparency from rock hand samples) are ~5% of the components, as in unit K2.
431 The claystone matrix forms the bulk of the lithological components. Characteristic
432 components of this layer are green, either equidimensional or horizontally elongated
433 clasts of chlorite (Fig. 6B), present throughout the whole layer, giving the characteristic
434 green colour of this unit. At the base of the unit (Fig. 6F, G), the green clasts usually
435 are equidimensional, being mostly subangular to angular grains.

436 Some reddish, small and irregularly shaped elements similar to but smaller than
437 the nodules from the unit K2 are present within the lower part of the layer (Fig. 6G).
438 Sparse small clast-like fragments composed of relatively large calcite crystals are also
439 present; sometimes these calcite crystals englobe small organic fragments (e.g., bones;
440 Fig. 6B), which may act as nucleus for the formation of calcite (pedogenic) nodules, as
441 observed in hand samples of unit K3. Bone fragments of fishes and tetrapods are
442 relatively sparse and without any preferential orientation, even oblique with respect
443 to the stratification. Ostracods are present, but scarce, being only abundant within the
444 infilling sediment of the mud cracks within unit K3 described in section 4.3.3 below.

445

446 4.3.2. Layered green mudstones with carbonate matrix

447 The facies composed of laminated/layered mudstones with a carbonate matrix
448 of unit K3 (Fig. 6H-J) has a much higher microfossil content than the massive
449 mudstones described above. The layers (0.5–1 cm-thick) are usually defined by
450 changes in the grain size (as observed in the thin sections, see below), and sometimes
451 are relatively poorly defined, though still distinguishable with appropriate lighting.
452 The general thickness of the whole deposits with these features is 2 to 3 cm.
453 Microscopic composition and grain size characterise this unit as fine, marly siltstones.
454 These rocks decay rapidly when put in water, and fresh breaks are covered with
455 yellow, carbonaceous dust.

456 These carbonate mudstones contain thin-walled ostracods, dominated by the
457 freshwater taxon *Darwinula liassica*. The high concentration of vertebrate remains in
458 this matrix is either due to accumulation over long time, sorting of elements by water
459 flows, or both. The general scarcity of sedimentary structures produced by water flows
460 (only some clusters of quartz grains likely accumulated due to transport have been
461 observed) may favour the hypothesis of accumulation over a relatively long period of
462 time. Further components are charophyte oogonia, fish scales, bone fragments, clay
463 peloids, and minute pieces of coal. It was reported (Urlich and Wild, pers. comm.
464 2020) that most large tetrapod bones and all skulls and skeletons were found in the
465 upper few centimetres of K3, which probably represents this facies of unit K3. Thus,
466 since layer K4a is erosive in some parts, the lower abundance of this facies with respect
467 to the massive mudstones described in section 4.3.1 above could be due to erosional
468 processes.

469 The thin sections of this laminated/layered facies (Fig. 6I, J) is characterised by
470 a micritic (carbonate mud) matrix. Quartz grains are sub-rounded and present a
471 heterogeneous distribution. In some parts they represent around 5% of the
472 components, whereas in some others they are accumulated, being ~50% (or even more)
473 of the components. In these accumulations, quartz grains define horizontal layers or
474 laminae (Fig. 6I, J). Of note, quartz grains are larger in the parts of the layer where they
475 are less abundant. Within the carbonate matrix, there seem to be sinuous,
476 interconnected lines defining the stratification (Fig. 6I). Bony remains are present, but
477 not very abundant; they are mostly elongated and parallel to the stratification (Fig. 6J).

478 Fish scales are numerous. Sparse, but very well identifiable, elongated fragments of
479 intense green colour that are parallel to the stratification are also present.

480

481 4.3.3. *Mud cracks in unit K3*

482 The massive non-carbonate facies of unit K3 (see section 4.3.1 above) displays a
483 network of mud cracks (Fig. 7) with two size classes: large cracks up to 2 cm wide (Fig.
484 7A), and innumerable small, closely-spaced, 1–5 mm wide cracks (Fig. 7B). These have
485 remarkably smooth walls, possibly indicating repeated flooding events. They
486 penetrate the whole unit, and are filled with the coarser marly sediment of the layer
487 K4a that is rich in ostracod shells (Fig. 7C-E). Also, the top surface of the greenish unit
488 K3 displays a relatively low relief, with shallow depressed areas, that can be of up to
489 a few centimetres of height. This relief is filled up by deposits of layer K4a, with the
490 contact boundary with the underlying greenish unit K3 being neatly defined (Fig. 5D,
491 E).

492 The large cracks are up to 2 cm wide and make up polygons in T-junction (see
493 Goehring et al., 2010) with a diameter of about 15–30 cm (Fig. 7A). Subordinated to
494 these large cracks, the small ones build a dense network (Fig. 7B). Observation of mud
495 cracks in present-day ponds (Fig. 8) allows inferring how those observed in unit K3
496 could have formed. Figure 8 shows Recent desiccation cracks that were flooded after
497 their generation. In an early stage of their opening, large polygons with T-junction are
498 formed, with subordinate, much smaller and narrower cracks covering large parts of
499 the polygons and being either straight or sinuous (Fig. 8A). The initial stages of their
500 infilling (Fig. 8B, C) show how the small, subordinate cracks are rapidly filled with
501 sediment, while the larger ones remain well visible, though with (apparently)
502 smoothed edges, thus actually also being filled with sediment. In later stages (Fig. 8D),
503 the largest mud cracks are still visible, even when the surface is covered with coarser
504 sediments and a new genesis of small cracks may be formed. In this sense, this shows
505 how mud cracks can be preserved over time even if the substrate is flooded (i.e.,
506 rehydrated) again and another (eco-) system is developed on this new subaquatic
507 setting (Fig. 8E-G). This would have been the case between the deposition of units K3
508 and K4, both formed in subaquatic settings and with a period of desiccation in
509 between, as discussed in section 6 below. In addition, the T-junction indicates that mud

510 cracks did not undergo many processes or periods of hydration-desiccation (Goehring
511 et al., 2010; Goehring, 2013), hence suggesting a prolonged drought period.

512 The thin-wall mud cracks are also visible in the thin sections (Fig. 7C-E). They
513 are characterised by vertical to oblique thin lines of darker carbonate sediment (that of
514 layer K4a), often with horizontal (lateral) ramifications. Towards the top of the layer,
515 the small mud cracks become more abundant, being closer to each other. The carbonate
516 infilling the cracks is micritic, and yields ostracods with the shells aligned to the walls
517 of the cracks, which are conspicuously abundant. In fact, the sediment that infilled the
518 cracks can be considered an ostracod packstone, also containing large quantities of
519 minute fish scales and teeth.

520 As a whole, the network of the desiccation cracks resembles patterns known
521 from palustrine deposits (Freytet and Plaziat, 1982; Freytet and Verrecchia, 2002;
522 Alonso-Zarza and Wright, 2010), with numerous, closely-spaced cracks of different
523 sizes and with curved walls (cf. Fig. 8). Although desiccation crack-like structures,
524 such as syneresis cracks, can also develop under water preferably with increased salt
525 content, these are much smaller and have a significantly different shape (Pratt, 1998),
526 not consistent with the structures identified in Kupferzell. Instead, cracks of this size
527 suggest that the water body completely dried out. In this sense, they could have been
528 generated either during a prolonged desiccation period or by a rapid drying in a
529 particularly hot climate (see further discussion in section 6 below).

530 Apart from the mud cracks, the infilling pattern of the unit K3 on the eroded,
531 channelized siltstones of the unit K2 may also indicate (longer) periods of desiccation
532 of the lake (Alonso-Zarza and Wright, 2010). Similarly, the preservation of *Gerrothorax*
533 skeletons also suggests long periods of decay of the carcasses, in line with long-term
534 subaerial exposure. Scavenging of the carcasses, even if direct evidence (e.g., bite
535 traces) have not been reported on this taxon, cannot be discarded for the disarticulation
536 and destruction of remains, especially considering the evidence of scavenging found
537 from this locality (Mujal et al., 2022; see also section 5.4 below). Of note, the laminated,
538 carbonate mudstones, which likely formed under a water flow, do not display
539 desiccation cracks. Therefore, the sediments composing this facies possibly did not
540 undergo long times of subaerial exposure, possibly indicating the existence of more

541 perennial pools or ponds within a generally desiccation period and pointing to a
542 patchy landscape (see sections 5, 6 and 7 below).

543

544 *4.4. Yellow and brown dolomitic marlstones (K4a-c)*

545

546 The upper part of the fossiliferous sequence in the Kupferzell lagerstätte
547 encompasses pale-coloured, yellow to brown marlstones (Figs. 5D, E, 9-11). Unlike the
548 underlying green mudstones, they were only present in the 500 m strip of the
549 excavation area, and their thickness and composition were subject to substantial lateral
550 change. Whereas the thickness of K4 is greater in the western part (but its end is not
551 exposed), it grades into a drift line towards the east, which contains fossil wood and
552 heavily reworked tetrapod bones. Whereas unit K3 is a relatively monotonous
553 stratigraphic succession (facies changes likely only occur laterally, see section 4.3
554 above), unit K4 can be stratigraphically divided into three well-differentiated sub-
555 units, from base to top: K4a, K4b, K4c.

556

557 *4.4.1. Pale yellow marlstones (K4a: 5–10 cm)*

558 The lower layer within the unit K4 consists of micritic, soft marlstones to
559 dolostones. They contain peloids/rounded clasts that are composed of siltstones, fine-
560 grained sandstones, and green claystones (Fig. 9).

561 This layer is composed of micritic calcite and is extremely rich in ostracods with
562 the long axis of the shells aligned in parallel to the stratification (Fig. 9B). Charophytes
563 are also relatively abundant, though not as much as the ostracods. Possibly, dissolved
564 and fragmented parts of these elements build part of the fine, muddy carbonate matrix
565 of this layer. Sub-rounded to rounded quartz grains represent the 2-5% of the
566 components of layer K4a, being markedly less abundant than in unit K3. Bone
567 fragments are more abundant than in unit K3, sometimes with sparry calcite covering
568 them at least partially (Fig. 9C). Round clasts or peloids composed of siltstones, very
569 fine-grained sandstones and claystones are present within the whole layer (Fig. 9D),
570 but they are more abundant and larger in the lowermost 2 cm of the layer (Fig. 9A).
571 These clasts correspond to eroded fragments from the underlying unit K3. The layer
572 also shows a heterogeneous distribution of components and relative abundance: in

573 some parts relatively irregular seams of dark carbonate (micritic) matrix are present
574 within a lighter carbonate matrix with more clasts and quartz grains (Fig. 9E). These
575 seams are roughly parallel to the bedding plain, and may reflect the channelized
576 structures observed in hand sample (Fig. 5D, E). In the upper part of the layer,
577 coprolites are also identified. Notably, below a relatively large coprolite there appears
578 to be a "precipitation shadow", with the sedimentary matrix being coarser, i.e., the
579 calcite crystals/fragments are larger than in the rest of the layer (Fig. 9F). In fact, in
580 this localised area below the coprolite, the matrix is more similar to that of the
581 lowermost part of the layer, with a coarser aspect. All in all, this whole layer was
582 formed under a water flow, as suggested by the disarticulated and oriented ostracod
583 shells, the presence of rounded clasts eroded from the unit K3, and the sinuous,
584 channel-like structures observed in the preserved sample including the whole K3-K4
585 sequence (Fig. 5D, E). Nonetheless, the deposition of layer K4a also underwent periods
586 of carbonate precipitation, likely during stagnation of waters and the development
587 (growth) of characeans, which may have built meadows (see section 6.2 below).

588 This unit yielded abundant and well-preserved ostracods (as observed in the
589 thin sections; Fig. 9), oogonia of charophytes, isolated fish remains (mostly scales),
590 small bone fragments, and larger tetrapod bones, including skulls and teeth. Some of
591 the best-preserved skulls of *Mastodonsaurus* and a few skeletons of *Gerrothorax* were
592 found in this horizon. Pseudosuchians and other terrestrial reptiles are mostly
593 represented by their teeth, and there are very few isolated bones from the
594 temnospondyls *Trematolestes* and *Plagiosuchus*. Even if less abundant, the tetrapods
595 from the unit K4 are still somewhat better preserved than those of unit K3, and most
596 *Gerrothorax* skeletons are articulated. This suggests lower water energy (which may be
597 in agreement with the lower abundance of quartz with respect to unit K3) and limited
598 or no exposure to reworking and weathering. Several skeletons of the plagiosaurid
599 *Gerrothorax* are preserved with osteoderms in natural articulation.

600

601 4.4.2. Light brown marlstones (K4b: 5–15 cm)

602

603 Layer K4b consists of pale brown carbonate mudstones with a generally
604 massive aspect (though a rough lamination or layering is observed in the examined

605 rock samples) and with darker round stains (Fig. 10A). Quartz represents <1% of the
606 components, only a few well-rounded grains are observed. Ostracods are present, but
607 they are much less abundant than in layer K4a. Their calcitic shells are irregularly
608 distributed. In some parts of the thin sections, ostracod shells are concentrated in
609 clusters, infilling oblique and sinuous to vertical irregular forms together with a
610 coarser carbonate matrix (Fig. 10B-F). These structures are also richer in quartz, being
611 slightly more abundant (2-5%) within this coarser matrix. The structures differ in
612 shape from the mud cracks observed within unit K3, being less penetrative and
613 relatively wider, with no lateral branching. Their walls have a relatively smooth shape
614 with no signs of cracking (Fig. 10B, C) as observed in mud cracks of K3, and they are
615 generally more oblique with respect to stratification. Ostracod shells within these
616 structures are oriented following the shape of the structure (Fig. 10C), indicating that
617 they were precipitated in them likely due to a water flow. As described in section 4.4.3
618 below, the sediment infilling these structures is more similar to that of layer K4c. All
619 in all, such structures most likely correspond to burrows, although some of them
620 outline more complex sinuous forms (Fig. 10B) that may not fit with this (tentative)
621 interpretation. If these structures were burrows, they could indicate periods of no
622 sedimentation and/or subaerial exposure, which may be in line with the erosive
623 nature of the subsequent layer K4c (see below). Charophytes and bone fragments are
624 sparse (Fig. 10D, E). A bivalve shell preserving its microstructure has also been
625 observed, suggesting favourable preservation conditions; therefore, the scarcity of
626 fossil of this layer could point to a reduced presence of biota.

627 Generally, layer K4b resembles the unit E7 from Vellberg-Eschenau (i.e., the
628 Anoplophora-Dolomite unit; see Schoch and Seegis, 2016). The top of this layer is a
629 sharp, erosive surface, with the overlying deposit being much coarser and richer in
630 quartz and bone fragments characteristic of layer K4c (Fig. 10F).

631

632 *4.4.3. Yellow marlstones with dolomitic concretions (K4c: 20 cm)*

633

634 In fresh state, this horizon of marlstones was reportedly yellow at its base and
635 brownish at the top (Wild, pers. comm. 2020). Layer K4c (Fig. 11) is somewhat similar
636 to layer K4a, but here ostracods are much less abundant, though still present (Fig. 11A).

637 Generally, the layer displays somewhat sinuous lamination, defined by slightly darker
638 lines or seams of micritic sediment (Fig. 11A, B). This denotes that this layer was
639 probably deposited under a water flow that partially eroded the previous layer (K4b;
640 which is in sharp contact, Fig. 10F), possibly after a period of no sedimentation or
641 desiccation (see section 6 below).

642 In the thin sections, quartz grains represent the ~10-15%, they are sub-rounded
643 to rounded. Small oval-shaped clasts of siliciclastic composition are present (Fig. 11B-
644 E). They are reminiscent to those observed in layer K4a, but much smaller and less
645 abundant. Charophytes seem slightly more abundant than in layer K4a. Bone
646 fragments preserved in 3D but also partially eroded are present (Fig. 11D, E). These
647 elements, together with the fragmented and abraded (due to erosion) ostracod shells
648 and charophytes (mostly oogonia) (Fig. 11F) as well as the seams and quartz grains
649 indicate water flow and transportation.

650 Large calcareous concretions, some of them containing vertebrate fossils, were
651 common in this layer (Urlichs, 1982). Teeth and skull bones of the large lungfish
652 *Ptychoceratodus* were found in this layer. The deposition of the brownish layer indicates
653 increased water cover, i.e., a renewed rise in groundwater. The tetrapod fossils from
654 this horizon have an orange-brown colour and are more heavily crushed than those of
655 layer K4a, except for those embedded in hard carbonate concretions. A partially
656 disarticulated skeleton of *Gerrothorax* stems from this horizon (SMNS 84786), with an
657 intact skull and hemimandibles located at a distance of 50 cm from the gently dissolved
658 postcranium. Disarticulated skulls of *Mastodonsaurus* probably form the most common
659 large finds in this layer, but there is not a single complete skull. Instead, several
660 excellent, fully articulated skulls of *Kupferzellia*, including the type specimen, were
661 embedded in this layer. Finally, a partial skeleton of the sauropterygian *Nothosaurus*
662 (SMNS 80266), in which most of the bones preserve bite traces, was found in a
663 concretion. In summary, this layer contains the best preserved specimens from the
664 Kupferzell lagerstätte.

665

666 4.5. *Anoplophora-Dolomite* (K5)

667

668 The unit K5 consists of pale yellow, micritic, massive dolostones. It is
669 lithologically very similar to horizon E7a at Vellberg-Eschenau (Schoch and Seegis,
670 2016). Yet unlike the latter deposit, where this unit produced abundant remains of
671 *Batrachotomus* (see Schoch and Seegis, 2016), it appears to have been less fossiliferous
672 at Kupferzell. Admittedly, the focus of attention during excavation was laid on the
673 fossil-rich units K3 and K4. Based on observations of Rupert Wild and Max Urlichs,
674 Schoch (1999) reported sparse remains from *Nothosaurus*, *Neusticosaurus* and
675 *Tanystropheus* from this layer. All these taxa represent purportedly marine fauna, and
676 thus may suggest an environmental change with more marine influence for the layer
677 K5 with respect from the underlying layers. Noteworthy, as aforementioned,
678 *Nothosaurus* remains have been found in the yellow-brown layer K4c, likely suggestive
679 of a progressive trend towards increasing marine influence.

680

681 **5. Vertebrate taphonomy**

682

683 Similar to the situation in Vellberg-Eschenau (Schoch and Seegis, 2016), bones
684 were often found accumulated in clusters (Wild, 1978a). They rarely formed relics of
685 single individuals (Schoch, 1999; Hellrung, 2003; Gower and Schoch, 2009) but rather
686 agglomerates of different specimens or even taxa. Articulated skeletons were almost
687 absent, except for the heavily armoured temnospondyl *Gerrothorax pulcherrimus*.

688 This somewhat irregular distribution of fossils indicates a patchy environment
689 (possibly a sabkha setting; see section 6 below) or a landscape composed of discrete
690 water bodies, most likely small lakes spread on a vast epicontinental platform with
691 intermittent connections to the sea. The patchiness of the original environment is also
692 suggested by the lateral changes of facies observed by Urlichs (1982) throughout the
693 region that houses the Kupferzell lagerstätte. Such environmental interpretation is
694 further supported by the sedimentological differences, mainly within the most
695 fossiliferous layers, between Kupferzell and Vellberg-Eschenau (see further discussion
696 in section 7 below). Another important agent on bone modification and distribution is
697 the presence of predators and scavengers roaming the area (e.g., Hungerbühler, 1998;
698 Augustin et al., 2020; Drumheller et al., 2020), which was the case in the Lower Keuper,

699 where bite traces are relatively frequent on the bones of large tetrapods (Mujal et al.,
700 2022).

701 Herein, we describe and interpret the main taphonomic features on the Lower
702 Keuper bone assemblage (Fig. 12), with a special focus on the units K3 and K4, the
703 most fossiliferous ones (Fig. 4). Generally, these features are not exclusive from a
704 specific unit or layer of those studied (K1 to K5), but if they are, it is specified. The
705 taphonomic features identified allow better defining the palaeoenvironmental settings
706 of Kupferzell, thus they are also discussed here where appropriate.

707

708 *5.1. Preservation and articulation*

709

710 The vertebrate bones and teeth from Kupferzell are exceptionally well
711 preserved (Fig. 12). This is for the most part due to their diagenetic impregnation with
712 sparitic calcite, giving the bones stability and facilitating their preparation from the
713 surrounding marly or clayey matrix (Fig. 12A). Yet, sometimes flakes of hard mineral
714 crusts are attached to the bone surface that are difficult to remove mechanically or
715 chemically. This is especially the case from the bones in layer K4c, many of them being
716 at least partially embedded in a calcite crust (Fig. 12B). In this sense, most of the bones
717 did not undergo a strong weathering process. Regarding the degree of weathering (see
718 definitions in Behrensmeyer, 1978; Fiorillo, 1988; Ryan et al., 2001), most of the bones
719 from Kupferzell are in the stage 1, with the bone surface showing incipient cracking
720 that does not penetrate the bone and/or initial flaking, and with most portions of the
721 surface being pristine (Fig. 12C-G). According to Wild (1980), weathering is mostly
722 observed on bones of *Bystrowiella* (erroneously identified as a therapsid by Wild, 1980).

723 Some dentigerous bones of *Batrachotomus* show more extensive flaking and
724 missing parts at their edges (Fig. 12E), which appears to indicate weathering stage 2.
725 Teeth of *Batrachotomus* sometimes show partial loss of enamel or are longitudinally
726 split, also pointing to weathering (Behrensmeyer, 1978). A similar network of cracking,
727 with a “mosaic”-like pattern (see Behrensmeyer, 1978: fig. 3), has also been observed
728 in some *Mastodonsaurus* bones (Fig. 12F). Such cracking also suggests more extensive
729 weathering, and could be linked to a long time of exposure under during drought

730 periods; in fact, the bone in Fig. 12F preserves matrix of both units K3 and K4, between
731 which an extensive network of desiccation cracks occurs.

732 Most of the bones are almost completely free from matrix, although some still
733 preserve part of it due to their fragility or because they correspond to associated
734 and/or articulated bones of a single specimen (Fig. 12A, B). Also, it is particularly
735 notable that most of the bones, even though isolated or disarticulated, are complete.
736 When parts of the bones are missing, it is usually because they were bitten/eaten
737 (Mujal et al., 2022) or parts of them were not recovered (or lost) during the salvage
738 excavation campaign. Only a few specimens seem to have been broken due to
739 transport, which is suggested by their weathered aspect that occurred prior to
740 fossilization.

741 Teeth of the pseudosuchian archosaur *Batrachotomus kupferzellensis* are very
742 abundant (Gower, 1999; Schoch et al., 2018; Mujal et al., 2022), particularly from the
743 unit K4, as evidenced by the yellow-brown colour of the sedimentary matrix remains
744 (Fig. 12H-K). The overwhelming majority of them consists of tooth crowns with hollow
745 bases, a feature that is due to resorption of the root during life (tooth replacement; Njau
746 and Blumenshine, 2006), which demonstrates that these teeth were shed by living
747 animals (Gower, 1999; Hungerbühler, 1998; Frey and Monninger, 2010). Only a few
748 teeth with intact roots were found together with jaw bones (Gower, 1999; Mujal et al.,
749 2022), suggesting that they had fallen out before the skeletal remains were covered
750 with sediment. Thus, the carcasses of *Batrachotomus* underwent some degrees of
751 decaying processes before their final burying (e.g., Fig. 12E). Similarly, skull bones of
752 *Batrachotomus* were found disarticulated but adjacent to each other (slightly scattered),
753 clearly corresponding to the same individuals (Gower, 1999; Gower and Schoch, 2009).
754 According to Voorhies (1969), skulls are not easily transported by currents, in contrast
755 to other elements such as ribs. This indicates that adjacent elements correspond to the
756 same individual, further denoting decaying processes, as suggested for *Gerrothorax*
757 specimens (see section 4.3 above). Considering the relatively good preservation of the
758 majority of *Batrachotomus* bones, showing none or few cracking and/or flaking of the
759 surfaces (Fig. 12E, L, M; see section 5.2 below), together with the fact that they are
760 disarticulated (indicating that they were buried after the disappearance of most, if not

761 all, the soft tissues), their preservation is considered between stages 2 and 3 in the
762 classification of Behrensmeyer (1978).

763 Bones of *Mastodonsaurus* likely underwent similar processes to those of
764 *Batrachotomus*. Some elements are also found in clusters (Schoch, 1999) but they are
765 completely disarticulated, indicating that the corpses underwent a certain period of
766 exposition before the final burial. In addition, the relatively high frequency of bite
767 traces (Mujal et al., 2022) indicates bone modification by scavengers or predators,
768 which can be important agents in the resulting bone assemblages (e.g., Hungerbühler,
769 1998; Njau and Blumenschine, 2006; Haynes et al., 2020). Most of the finds consist of
770 single, sometimes primarily incomplete bones. The few bone clusters identified
771 (Schoch, 1999) consist of groups of vertebrae or sets of shoulder girdle bones belonging
772 to single individuals of *Mastodonsaurus*. A giant skeleton of *Mastodonsaurus* (SMNS
773 81310), with a skull of some 120 cm length and a 145 cm long mandible was recovered
774 from the green unit K3 (Schoch, 1999). This find includes a complete sequence of trunk
775 vertebrae and ribs, some of which are covered with bite traces (Mujal et al., 2022).

776 Most temnospondyl skulls were found disarticulated from the mandibles, but
777 are often preserved in close proximity. The only exception is a *Mastodonsaurus*
778 specimen (SMNS 54677) where the jaws are still firmly articulated with the skull
779 (Schoch, 1999: fig. 8); this was found in the top of unit K4a. Isolated skull bones of
780 temnospondyls were abundant, and at least one totally dissociated skull of
781 *Mastodonsaurus* (SMNS 80878) was recovered. As in the case of *Batrachotomus*, this is in
782 agreement with a decay process of corpses, indicative of an exposure period of time
783 (Behrensmeyer, 1978). Similarly, a totally disarticulated, yet almost complete skull roof
784 of the large dipnoan *Ptychoceratodus serratus* was recovered from the yellow-brown
785 unit K4c. The single bones were found far from another (Schultze, 1981), suggesting
786 some kind of transport.

787 Only the yellow-brown layer K4c, forming the top of the Untere Graue Mergel
788 (UGM) just below the Anoplophora-Dolomite (unit K5), produced a few articulated or
789 semi-articulated skeletons of the plagiosaur *Gerrothorax* (e.g., Hellrung, 2003; Fig. 12B).
790 Probably, the dermal armour plates of this temnospondyl prevented a higher degree
791 of disarticulation as occurred in the other taxa. Also, the fact that partial and
792 disarticulated skeletons of *Gerrothorax* have been found in other layers (e.g., Fig. 12A),

793 suggesting transport (see section 5.3 below), possibly shows that layer K4c formed
794 under energy conditions lower than other layers, even though water currents are
795 inferred for layer K4c (see section 4.4.3 above).

796 Another particular specimen is a disarticulated, fragmentary skeleton of the
797 aquatic sauropterygian reptile *Nothosaurus* (SMNS 80266), usually found in marine
798 deposits. It was found in the layer K4c, with most of the bones embedded in hard
799 calcite concretions, sometimes with some fish scales as well. The skeleton preserves
800 only bones of the posterior part of the trunk: vertebrae, pelvic girdle, and ribs (dorsal,
801 sacral, and one fragmentary caudal). The presence of bite traces on several bones
802 (mostly on ribs) of this partial skeleton indicate that scavengers were a further
803 taphonomic agent of this specimen, which was possibly wash out from a
804 marine/coastal setting (see section 6 below).

805 Except for rare patches of a few ganoid scales in mud crack fillings of the green
806 unit K3, no associated fish remains were found. Obviously, no articulated skeletons of
807 fishes are preserved at the Kupferzell site, because at least some accumulations of
808 ganoid scales would have been recognised during the excavation, if present.

809 In summary, there are some major differences between units K3 and K4. In K3,
810 vertebrate fossils are more abundant, but usually disarticulated and isolated, though
811 including also some bone clusters suggesting the presence of water flows that
812 accumulated different elements (Fig. 12A). In K4, fossils are less abundant, but their
813 preservation is better in terms of bone weathering and articulation (Fig. 12B). This
814 indicates a decrease of water energy from K3 to K4, with a clear interruption in the
815 development of the settings between the two units, marked by a likely prolonged
816 period of desiccation; the chronology of events is discussed in section 6 below. Besides
817 this, bones from these two units change in colour, with those of K3 (Fig. 12A, C) being
818 darker than those of K4 (Fig. 12B, D). A remarkable feature of the bones (and more
819 generally clasts, including also coprolites) from unit K4 is that they have a precipitation
820 rim of sparry calcite. This rim may not surround the entire bone or clast, but it is at
821 least present in the stratigraphically lower surface of each element (e.g., Fig. 9F). This
822 indicates a precipitation phase during diagenesis, with a washing of the carbonate of
823 the matrix that (re-) precipitated around the clasts and in the likely diagenetic cracks

824 generated within the layer. This crust would have also prompted a better preservation
825 of the elements in unit K4 (Fig. 12B, G).

826

827 5.2. *Fracturing*

828

829 All the fracture types defined by Haynes (1983) (see also Ryan et al., 2001;
830 Haynes et al., 2021) have been identified in the Kupferzell bones. These include:
831 longitudinal, spiral (green) and transverse/compression fractures (Fig. 12C, D, G, L,
832 M). These fractures are generally considered green, i.e., they occurred (relatively) soon
833 after the death of the individuals. The peculiar mosaic-like pattern of fracturing of
834 uncertain origin identified by Behrensmeyer (1978) is also present in some Kupferzell
835 bones (Fig. 12F). Some other fractures from indeterminate causes, as well as fractures
836 due to collecting and specimen manipulation, have also been identified.

837 A particular type of fracture morphology and arrangement is that observed on
838 the ends of limb bones and on rib heads, i.e., in elongated bones. These fractures are
839 semi-circular, with the concave side facing towards the outer part of the bone; they
840 often occur in multiple sets, being aligned and thus giving a stepped aspect to the
841 fractured portion (Fig. 12C, D, L). Such fractures were probably generated by a
842 differential compactness of the bone, being higher in the midshaft (i.e., more dense)
843 than in the ends (see Hugi and Scheyer, 2012). This is indeed the case for the
844 *Batrachotomus* teeth still preserving at least part of their roots, which are hollow and
845 thus collapse easily.

846 Spiral and oblique fractures, also showing right angle offsets, all interpreted as
847 green fractures (Haynes, 1983; Haynes et al., 2021; see also Britt et al., 2009) (Fig. 12G,
848 M), are commonly found on ribs of *Mastodonsaurus*, as well as on *Nothosaurus*, and in
849 some bones of *Batrachotomus*. Other fractures may have also occurred due to
850 trampling, with bones broken in different parts, but with fractured surfaces clearly not
851 being recent (i.e., surfaces are slightly smoothed, and sedimentary matrix and/or
852 calcite crystals are usually covering them). Other fractures that probably occurred due
853 to trampling are sets of radial fractures that widen towards the central point (Fig. 12F),
854 suggesting that pressure was applied on the widest point or area of the fracture. These

855 radiating structures are especially well seen in some platy bones, i.e., those with
856 relatively large surfaces.

857 Other relatively common fractures, well observed in some plagiosaur (e.g.,
858 *Gerrothorax*) skeletons, seem to have been produced due to desiccation. This is in
859 agreement with the palaeoenvironmental setting indicated by the presence of
860 relatively abundant desiccation cracks on the layers, especially penetrating on the unit
861 K3 and generated before the deposition of the unit K4. Similarly, this also supports the
862 long period of decay of carcasses interpreted for *Gerrothorax* (see section 4.3 above).

863 Some of the thin interclavicae of *Gerrothorax* were embedded in an incomplete
864 state, often with their anterior part missing, the breakage planes being almost planar
865 and straight to slightly curved. In *Plagiosuchus*, some fragments of platy shoulder
866 girdle bones were found widely separated from each other but could be fitted together
867 again. The fragments differ partly in colour, suggesting that the bones were broken
868 prior to their burial in the sediment, and then being again reworked and hydraulically
869 concentrated together with fresh bones in the lagerstätte.

870 Teeth of *Batrachotomus* are sometimes transversely dissected by calcite-filled
871 cracks, up to eight parallel, sometimes bifurcating cracks having been observed (Fig.
872 12H, I). Interestingly, fractures are generally neat: even if the broken parts of the teeth
873 are separated some millimetres by the infilling sediment, they fit well together. In most
874 cases, fractures are transverse and/or oblique to the tooth long axis (Fig. 12H, I), but
875 some teeth are longitudinally split with the two halves slightly displaced; in all cases
876 they were infilled with sediment and diagenetically cemented with calcite. They could
877 have been generated due to desiccation, though this cannot be confirmed. Some
878 cracked teeth have the broken fragments displaced (slightly scattered or spread, like if
879 they had “exploded”) from their original position (Fig. 12J, K), most likely because
880 they were trampled after being shed. In summary, teeth could have been broken due
881 to desiccation, due to trampling or both. In tusks of *Mastodonsaurus*, this phenomenon
882 is much rarer, and there are never more than 2-3 calcite-filled cracks.

883

884 5.3. Orientation and sorting

885

886 Except for one specimen (SMNS 54675, the most 3D-preserved), all other skulls
887 of *Mastodonsaurus* were found facing with their dorsal side up. Their longitudinal axis
888 was SE-NW-oriented, and the heavy occiput pointed towards the southeast (Urlich,
889 pers. comm. 2015). As long bones often exhibited also a SE-NW-orientation (Wild,
890 1978a), these observations point to alignment of the bones following southeast-bound
891 currents. Together with skulls, other plate-like bones of temnospondyls, such as
892 interclavicles, are especially abundant, also pointing to their enhanced transportability
893 with respect to bones with non-platy morphologies. Some platy bones were found in
894 a more or less vertical position (Wild, 1978) (cf. Fig. 12F), sometimes being broken
895 likely due to compaction. They were possibly washed into mud cracks, as suggested
896 by some vertically orientated small bones that were lying in such cracks during the
897 preparation of fossiliferous sediment blocks.

898 Evidence of transport is also suggested by the accumulation of some bones of
899 different individuals and taxa in clusters, especially in the unit K3 (Wild, 1980). Some
900 bones, including partial skeletons in this unit (e.g., Fig. 12A) are chaotically oriented,
901 being oblique with respect to stratification. Especially in the case of partial skeletons,
902 represented by clusters of bones of disarticulated skeletons, the orientation of the
903 elements (which are often fragmented but preserving delicate details; i.e., fractures)
904 indicates transport of the skeletons or decaying carcasses in a mud flow (e.g., Britt et
905 al., 2009). The muddy matrix would have protected bones from erosion or abrasion,
906 yet they could have been broken due to impacts with other bones or other hard clasts.
907 Due to transport, some elements would have been lost, and when the mass transport
908 stopped, the bones would have remained in their position, with no preferential
909 orientation (Fig. 12A), in a rather cohesive muddy matrix. Outside of unit K3, the
910 cranial bones of the giant lungfish *Ptychoceratodus* were found scattered in a relatively
911 large area of the yellow and brown layers K4b and K4c (Schultze, 1981).

912

913 *5.4. Predation/scavenging and bioerosion as taphonomic agents*

914

915 *5.4.1. Predation and scavenging: bite traces*

916 Many bones from the Kupferzell site are covered by bite traces (Mujal et al.,
917 2022). This feature was already mentioned by Wild (1978a, 1978b, 1979, 1980). Schoch

918 and Seegis (2016) reported bones with bite traces from the equivalent layers of the
919 Vellberg-Eschenau site, and more recently, Mujal et al. (2022) described the whole bite
920 trace assemblage for the UGM, with around 95% of the bitten bones coming from
921 Kupferzell.

922 At Kupferzell, bite traces have been regularly identified on bones of four
923 tetrapod taxa: *Mastodonsaurus*, *Plagiosuchus*, *Batrachotomus*, and *Nothosaurus* (Mujal et
924 al., 2022). In addition, there is a single evidence of a bite trace on a rib of the
925 chroniosuchid *Bystrowiella*. Although *Gerrothorax* is by far the most abundant tetrapod
926 genus, only a single bone fragment of this temnospondyl contains potential bite traces.

927 According to Mujal et al. (2022), six main types of bite traces can be
928 distinguished, which include the following ichnotaxa (see Mikuláš et al., 2006;
929 Jacobsen and Bromley, 2009; for taphonomic terminology see Binford, 1981 and
930 D'Amore and Blumenschine, 2009, 2012 for taphonomic terminology; for additional
931 classifications and terms, e.g., dentalites, see Hunt and Lucas, 2021): *Knethichnus*
932 *parallelum* Jacobsen and Bromley, 2009, corresponding to parallel grooves generated
933 by denticles of ziphodont teeth; *Nihilichnus nihilicus* Mikuláš et al., 2006, round to oval,
934 sometimes bisected, punctures; *Linichnus serratus* Jacobsen and Bromley, 2009, grooves
935 with serrated margin, with a range of linear morphologies, from straight to strongly
936 curved (hook-shaped); *Brutalichnus*, recorded by two clearly differentiated
937 morphotypes, both with roughly serrated margins and reaching cancellous bone (large
938 round- to oval-shaped hole, and V-/triangle-shaped trace at the bone margin);
939 *Machichnus*-like, corresponding to small hacks (punctures plus short grooves) found
940 in dense clusters.

941 Most of the bite traces are found on bones of *Mastodonsaurus*. The second taxon
942 ranked by the quantity of bitten bones is *Batrachotomus*, while on other taxa bite traces
943 are not frequent. In the case of the partial skeleton of *Nothosaurus* (SMNS 80266,
944 corresponding to a single individual), most of the bones contain bite traces, suggesting
945 a complete exploitation of the carcass, as it is the case of *Mastodonsaurus* (see discussion
946 in Mujal et al., 2022). The overwhelming majority of bite traces can be attributed to
947 *Batrachotomus*, on account of the serrated imprints of ziphodont tooth carinae on the
948 bones (i.e., *Knethichnus parallelum*, and *Linichnus serratus* as well; Mujal et al., 2022).
949 Biting traces on heads of limbs suggest that *Batrachotomus* preyed even on large

950 *Mastodonsaurus* specimens (Mujal et al., 2022). In summary, both scavenging and
951 predatory behaviours (as well as cannibalism) can be inferred for *Batrachotomus*.

952 In addition to scavenging and hunting large temnospondyls, there is also
953 evidence for cannibalistic habits of *Batrachotomus*. This is indicated by the relatively
954 large number of ribs and pelvic girdle bones with *Knethichnus parallelum* and *Linichnus*
955 *serratus* biting ichnotaxa. Considering the similar biting patterns to those found on
956 bones of *Mastodonsaurus* and the concentration of the traces to the trunk and pelvic
957 regions, the bite traces on bones of *Batrachotomus* indicate scavenging rather than
958 predation (Mujal et al., 2022). The frequency and associations of bite traces referred to
959 *Batrachotomus* are most similar to those produced by extinct and extant crocodyliforms
960 (Njau and Gilbert, 2016), indicating a conserved feeding ecology in the pseudosuchian
961 lineage (Mujal et al., 2022).

962 Several bones with bite traces come from in-between the green (K3) and yellow
963 (K4a) layers, indicating that bones remained exposed for a relatively long time after
964 the formation of the green layer (unit K3) and the sedimentation of the yellow one (unit
965 K4), probably during relatively long drought period(s), as the large mud cracks
966 suggest (see section 4 above). This preservation of bones between two layers is also
967 suggestive of trampling, as occurs in Recent bone assemblages (Haynes et al., 2020).

968 Trampling is not only suggested by some fractured bones (see section 5.2
969 above), but also by those embedded between layers K3 and K4a (Fig. 12F, N, O). In this
970 case, bones (and some teeth) were partly buried within layer K3, with orientations that
971 would not have occurred under normal sedimentary processes. Their odd positions
972 suggest trampling by tetrapods as most plausible explanation. This hypothesis is based
973 on similar orientations of trampled bones of Recent elephants, some of which being
974 subsequently scavenged by carnivores (Haynes et al., 2020). Some of the Kupferzell
975 bones show similar features and orientations, such as the *Mastodonsaurus* humerus
976 SMNS 81171 (Fig. 12O) and femur SMNS 81169, both containing relatively abundant
977 bite traces produced by *Batrachotomus* (Mujal et al., 2022) and also embedded between
978 units K3 and K4. Additional elements of *Mastodonsaurus* preserve matrix that indicates
979 their embedding between two layers, such as a scapulacoracoid (Fig. 12F) and a fang
980 (Fig. 11N). The fang preserves round holes likely due to chemical weathering whereas
981 the scapulacoracoid contains cracks suggesting bone flaking probably caused by

982 desiccation (Behrensmeyer, 1978). These bones embedded between two layers indicate
983 long times of exposure. This would explain also the large mud cracks and the change
984 in colour of the sediments, suggesting some sort of chemical change in the local lake
985 environment.

986

987 5.4.2. Inferred corrosion by gastric acids

988 The two most fossiliferous units at Kupferzell (K3 and K4) produced a number
989 of comparatively large vertebrate remains that are heavily worn. Firstly, some lungfish
990 tooth plates (*Ptychoceratodus*) still attached to their (incomplete) jaw bones have lost all
991 of the enamel (Fig. 12P). Compared to complete specimens with their enamel layer
992 intact, the shape of these lungfish tooth plates appears to be altered strangely.
993 Secondly, in a number of temnospondyl vertebrae (including some smaller
994 *Mastodonsaurus* vertebrae, e.g., SMNS 81230, 84160, and uncatalogued specimens) the
995 cortical bone layer is partly or totally missing (Fig. 12Q, R), or the vertebrae are just
996 consisting of rounded chips of the cancellous bone. These features suggest that these
997 lungfish teeth and temnospondyl bones were digested, so that gastric acids would
998 have caused strong chemical corrosion of the phosphatic substance of these elements.
999 It is unclear if the corroded elements were excreted through the digestive tract, encased
1000 in coprolites), or if they were orally expelled as regurgitalites (in general, bromalites;
1001 see Gordon et al., 2020). At least the dipnoan tooth plates and jaw bones are completely
1002 devoid of any traces of coprolite substance, so the latter explanation seems more
1003 plausible for them. Similar pellets of fairly complete skeletons have also been
1004 recovered from Vellberg-Eschenau (Schoch and Seegis, 2016; Sues et al. 2020). It still
1005 remains unclear whether the producers of such bromalites (mostly regurgitalites) were
1006 relatively large *Mastodonsaurus*, *Batrachotomus* or both. Since this behaviour has
1007 already been described in pseudosuchians (Gordon et al., 2020), being a further
1008 evidence of shared habits with crocodylians, at least some of the regurgitalites could
1009 have been produced by *Batrachotomus* (see also discussion in Mujal et al., 2022).

1010 Coprolites of all sizes (up to 7 cm large, mostly 0.5–2 cm) were abundant and
1011 may contain fish (actinopterygian) scales and even jaws. Most of them are oval-shaped,
1012 some have an even more elongated shape; in cross section, they are circular to oval.
1013 The largest ones were probably produced by *Mastodonsaurus*. The presence of

1014 coprolites indicates that their producers inhabited (or at least frequently roamed) the
1015 area (see also Schoch and Seegis, 2016). Considering the fragmentary nature of the so
1016 far few bone and tooth remains found within coprolites, the previously mentioned
1017 bones and teeth with signs of corrosion (much larger than the average size of the
1018 coprolites) (e.g., Fig. 12O-R) were probably regurgitated.

1019

1020 **6. Depositional history**

1021

1022 The sedimentological features of the most fossiliferous units of Kupferzell (K3
1023 and K4), together with their palaeontological contents, allow a reconstruction of the
1024 depositional history (Fig. 13). We have identified two main phases within the
1025 fossiliferous units. It should be noted that these layers are subject to lateral variation
1026 over hundreds of metres (Urlichs, 1982). Despite this variation, a general stratigraphic
1027 stacking pattern is still recognisable within the Untere Graue Mergel (UGM), and thus
1028 correlations are possible (Fig. 2). Therefore, such deposits might reflect basin-scale
1029 processes, as it has been identified at the level of the major units composing the Lower
1030 Keuper (Erfurt Fm.), at the scale of the Central European Basin (CEB) (e.g.,
1031 Pöppelreiter and Aigner, 2003, 2008; Franz et al., 2013; Nitsch, 2015).

1032 The Kupferzell units were deposited in a distal floodplain that underwent
1033 different episodes of drought and flooding by the sea from the southwest, similar to
1034 the depositional history at Vellberg-Eschenau (Schoch and Seegis, 2016). In Kupferzell,
1035 two main phases of lacustrine (or lacustrine-like) deposition building up the fossil
1036 lagerstätte (units K3 and K4) are identified (Fig. 13). They are preceded by an interval
1037 of highly changing environments (from marine to peat lake or swamp) in a generally
1038 more open setting (units K1 and K2). After the sedimentation of the fossil-rich units
1039 K3 and K4, a more open (marine) setting rich in carbonate (unit K5) was established.

1040

1041 *6.1. Rock sequence at the base of the lagerstätte*

1042

1043 The base of the studied sequence is consistent with the widespread, typical
1044 facies of the Lower Keuper in northern Württemberg, traditionally known as
1045 “Lettenkohle” (see also Brunner, 1973; Schoch and Seegis, 2016). The dark coaly

1046 mudstones (K1) were probably deposited in a vast swampy area, covered by a rich
1047 hygrophilic vegetation and with intermittent marine or fluvial influence (Nitsch, 2015).
1048 The latter prompted inputs of water flows with transportation of plant debris that
1049 contributed in the eventual formation of coal. These deposits generally represent a
1050 lagoonal-estuarine-lacustrine water system in which tetrapod faunas existed, though
1051 not as taxonomically diverse as in units K3 and K4. In most of these deposits, tetrapod
1052 remains were not accumulated and are therefore much less abundant than in the
1053 lagerstätten localities. Nonetheless, as suggested for freshwater peat swamps
1054 associated with salt-marsh estuaries (Behrensmeyer and Hook, 1992), taphonomic
1055 biases in the preservation of tetrapods possibly exist for unit K1. Generally, deposits
1056 of unit K1 might have formed during a period of increasing accommodation,
1057 prompting the accumulation of plant debris (e.g., Pöppelreiter and Aigner, 2003 and
1058 references therein). At any rate, they represent a setting with extensive plant growth.

1059 The swampy, densely vegetated environment was succeeded by settings with a
1060 stronger marine influence. A relatively abrupt change in the basin, possibly prompted
1061 by a rapid marine transgression, is indicated by bivalves that tolerated saline waters
1062 (*Myophoria transversa*). At Kupferzell, these are embedded in hard siltstones (K2),
1063 which probably correlate with coquinas with the same bivalve faunas in closely
1064 located sections (Urlichs, 1982; Hagdorn et al., 2015).

1065 This marine incursion probably did not last long, as the presence of oxidised
1066 (reddish) ironstone nodules and freshwater ostracods (*Darwinula*) within unit K2
1067 indicates. In addition, the presence of root traces denotes stabilization of the substrate.
1068 Eventually, probably responding to the regression of the sea, the silty deposits of unit
1069 K2 were overrun by water flows originating in terrestrial environments that partially
1070 eroded them and left the distinctive, N-S oriented channels reported by Wild (1980)
1071 and Urlichs (1982).

1072

1073 6.2. Lake Kupferzell K3

1074

1075 The first lake deposit is documented by the basal sequence of green mudstones
1076 (K3). The relatively silty facies at Kupferzell-Bauersbach is present in a 2×2 km area,
1077 with a 0.5×0.1 km large belt of high bone accumulation in its centre. This is embedded

1078 in a larger occurrence of green mudstones covering some 6×4 km size. To the north
1079 and east, the green mudstones grade into grey claystones, indicating a somewhat
1080 deeper and calmer depositional environment. The whole setting suggests a water body
1081 that was shallower to the west and deeper to the north and east; its further extension
1082 remains unclear. A rich fish fauna was found in microfossil samples northeast of the
1083 Kupferzell excavation ("Gasleitung" site, Fig. 1B), confirming the same lake fauna for
1084 the grey mudstones.

1085 We interpret the green mudstones as littoral facies of a lacustrine system (Fig.
1086 13). The silt, a relic of the sediments that formed unit K2, was probably transported by
1087 rivers into the basin, as well as some of the vertebrate bones (e.g., *Bystrowiella*). It
1088 contains characeans and ostracods (see Urlichs, 1982) that indicate well-aerated and
1089 clear water, probably housing characean meadows, and providing excellent living
1090 conditions for diverse fishes and lake bottom-dwelling predators (*Gerrothorax*). The
1091 abundance of characeans indicates a water depth of less than 10 m (Cohen and Thouin,
1092 1987). The association of characeans and *Darwinula* suggests oligo- to mesotrophic
1093 conditions, probably influenced by the intense plankton-feeding activity of the
1094 ostracods.

1095 The dichotomy of facies of unit K3 (massive and non-carbonate *vs.* laminated
1096 and carbonate) may be explained by its transition from unit K2: the laminated facies
1097 contain much more carbonate than the massive ones, and the quartz grains are also
1098 usually larger and more angular in the laminated facies, being accumulated in
1099 horizontal bands that define such lamination. This type of facies (which is less
1100 abundant than the massive one) may represent episodes of more energetic conditions,
1101 reminiscent of those during the deposition of unit K2, within the generally low water
1102 flow that characterised the sedimentation of unit K3. The decrease of quartz grain size
1103 from base to top in sequences of the massive facies type of unit K3 is also relevant,
1104 because this further documents the energy decrease from unit K2 to unit K3. The low
1105 content of carbonate in the massive facies would indicate less-aerated waters and thus
1106 explaining the lower number of characeans observed in the thin sections. The reddish
1107 nodules at the base of the massive facies of unit K3, which are reminiscent to those of
1108 unit K2, also denote the transitional nature between the two units.

1109 Freshwater conditions are suggested for K3 by the environmental affinities of
1110 the preserved taxa (e.g., dominance of *Darwinula liassica*) and the absence of euhaline
1111 bivalves (e.g., *Myophoria*, *Bakevellia*). However, the occurrence of euryhaline ostracods
1112 (*Speluncella teres* and others), albeit rarer than the freshwater taxon, suggests that
1113 salinity may have fluctuated. It is possible that *Speluncella* was restricted to certain
1114 layers, but because of the absence of laminae and the generally low thickness of unit
1115 K3, resolution is not fine-scaled enough to test this hypothesis. Environmental
1116 fluctuations are further suggested by the microanatomical analysis of bone growth in
1117 *Gerrothorax*, and have been interpreted as caused by periodic changes in salinity
1118 (Sanchez and Schoch, 2013).

1119 Urlichs (1982) reported that the sediments of unit K3 infilled the channels and
1120 gullies on top of the siltstones of the unit K2; we refer to the water flow that produced
1121 the gullies as *Event 1* (see Fig. 13 for an overview of events). These must have been
1122 caused by water currents flowing in N-S orientation, an observation roughly consistent
1123 with the NW-SE orientation of elongated elements reported by Wild (1980). The
1124 deposition of unit K3 occurred after substantial erosion of different sediments in the
1125 vicinity, because it contains clasts of various composition; these are predominantly
1126 composed of claystones, although the presence of quartz grains and reddish nodules
1127 (the latter only at the base of the unit) like those from the unit K2 is remarkable, further
1128 denoting a transition from units K2 to K3, though with a relatively sharp drop of
1129 quartz grains (Fig. 3). Considering the similar composition (but with different
1130 proportions of quartz content) between units K2 and K3, the initial deposition of unit
1131 K3 was part of *Event 1*, representing its latest phase. Considering the rather sterile
1132 sediment in the lower part of K3, the water flow is unlikely to have transported
1133 carcasses or single bones of vertebrates in larger quantities – the numerous fossils from
1134 the green mudstones stem from the uppermost horizon of K3. The water currents
1135 might have been produced by inflowing freshwater from rivers into the local
1136 Kupferzell basin, where a freshwater lake (K3) with characeans and ostracods was
1137 established (*Event 2*).

1138 The poor carbonate content of the dominant facies of unit K3 suggests that this
1139 lake was constantly fed by freshwater influx by a river large enough to produce
1140 currents that were able to align long bones and skulls in the putative NW-SE flow

1141 direction. In this regard, deposits of unit K3 most likely correspond to the infilling and
1142 eventual plugging of the gullies generated on top of unit K2, thus showing a sequence
1143 of energy decrease from K2 to K3. This may also explain why the upper part of K3 is
1144 much richer in fossils than the lower part, with a decrease of the water energy
1145 throughout the sedimentation of K3, conditions would have been more favourable
1146 towards the top of the unit.

1147 Fluctuations of salinity, as suggested by the mixed ostracod fauna and the
1148 histological variation of *Gerrothorax* (Sanchez and Schoch, 2013) could stem from
1149 eroded brackish sediments in the vicinity or from salt aerosols (Nitsch, 2003).
1150 Alternatively, it could simply reflect occasional input from a nearby brackish water
1151 body. The latter alternative is supported by the sections to the SW of Kupferzell
1152 (Schwäbisch Hall-Hessental, Michelbach an der Bilz, Gaildorf-Schleifrain) in which
1153 lagoonal deposits dominate the top of the Untere Graue Mergel sequence. In addition,
1154 the region northeast of the Kupferzell area also harboured a lagoon, as preserved in
1155 the quarry at Kirchberg an der Jagst.

1156 In a subsequent *Event 3*, a diverse fish fauna was established in Lake K3. This
1157 fauna formed a complex trophic web similar to the one known from Vellberg-
1158 Eschenau (Schoch and Seegis, 2016). At Kupferzell, it includes three sharks, eight
1159 actinopterygians, one actinistian and two lungfishes. The preserved littoral zone was
1160 inhabited by two main temnospondyl predators, *Gerrothorax* and *Mastodonsaurus*. The
1161 dominance of *Gerrothorax* is noteworthy, as this taxon was widespread and
1162 geologically long-lived but usually not preserved with large samples (Schoch and
1163 Witzmann, 2011). Its abundance in the K3 fauna indicates excellent living conditions
1164 and little competition by other large predators. This heavily armoured bottom dweller
1165 was evidently not an able swimmer and therefore bound to habitats with a constant
1166 supply of prey, most likely fishes in the size range of polzbergiids (*Serrolepis*,
1167 *Dipteronotus*) and redfieldiids. In the recently studied lake deposits at Vellberg (units
1168 E5 and E6; Schoch and Seegis, 2016), *Gerrothorax* was rare, either because the preserved
1169 environments were less favourable for that taxon or because of competition by a more
1170 diverse temnospondyl fauna (*Callistomordax*, *Plagiosuchus*, *Kupferzellia*, *Trematolestes*).
1171 *Gerrothorax* and the ostracod *Darwinula*, which was unable to produce aestivating eggs,
1172 required a constant water body for their life cycle and thus suggest a perennial lake.

1173 The abundance of high-bodied polzbergiid fishes (*Serrolepis*, *Dipteronotus*) suggests a
1174 habitat that was differentiated at a small scale, possibly influenced by characean
1175 meadows and a locally structured lake floor.

1176 The abundance of single bones was probably caused by a combination of
1177 factors: (1) disarticulation by predators (particularly *Mastodonsaurus* and possibly
1178 *Batrachotomus*), (2) water currents (sorting with preference of platy elements) and (3)
1179 accumulation over longer time, suggesting low rates of sedimentation.

1180 Lake K3 eventually dried up in the Kupferzell area (*Event 4*), resulting in deep-
1181 reaching cracks and a hardened surface, on which numerous skulls and at least one
1182 partial, giant skeleton of *Mastodonsaurus* were found, as well as partial skeletons of
1183 *Batrachotomus*. Many of these finds still have green mudstones on their lower and
1184 yellow marlstones on their upper sides. The richness of skeletal material on this surface
1185 probably represents a mass mortality event, which attracted terrestrial predators such
1186 as *Batrachotomus* (Wild, 1980). These large predators probably caused the
1187 disarticulation of the temnospondyl skeletons as well as the trampling phenomena
1188 reported in sections 5.2 and 5.4 above. The deep cracks filled with yellow-brown
1189 sediment and abundant ostracods of layer K4a were generated in the depositional
1190 phase after the formation of unit K3 (*Event 5*), as also suggested by the compositional
1191 change between units K3 and K4, indicating an interruption of sedimentation and the
1192 settlement of different environmental or climatic conditions. Subsequent inundations
1193 of the mud plain successively covered the bones with a calcareous mud layer and
1194 prevented them from getting weathered. Such phases of inundation and drying are
1195 indicated by *Batrachotomus* teeth that show many parallel, calcite-cemented cracks (Fig.
1196 11H-K). Conceivably, there were a few cycles of inundation-desiccation, this can be
1197 explained by the shape of the mud cracks, which have a T-junction geometry rather
1198 than Y-junction (see discussion in: Goehring et al., 2010; Goehring, 2013; compare Figs.
1199 7A, B and 8).

1200

1201 6.3. Lake Kupferzell K4

1202

1203 The K4 sequence formed in a shallow, carbonate-rich lake environment that
1204 housed a rich benthos. The ostracod *Darwinula* was abundant, accompanied by the 14

1205 aforementioned fish taxa, essentially the same as in K3. The yellow carbonate mud that
1206 filled the desiccation cracks on the topmost surface of K3 is consistent with the
1207 subsequently deposited marlstones (Figs. 5D, E, 7). A major difference between units
1208 K3 and K4, with the mud cracks separating them and a sharp change in composition
1209 (especially regarding the content of carbonate and ostracods, which is much higher in
1210 K4) is observed. This marks an environmental change between the two units. We
1211 conclude that the depositional regime changed after *Event 4* (a prolonged desiccation
1212 period), when a mud richer in carbonate, ostracods and microvertebrates, but equally
1213 rich in characeans, was deposited.

1214 The base of the K4a sequence includes stacked, 5–20 cm wide channel-fills that
1215 indicate migrating gullies in the early phase of deposition. Such channels might have
1216 been caused by water stemming from an inflowing river or small delta (*Event 5*). The
1217 sediment contains peloids of green mudstones and siltstones, equivalent to that from
1218 unit K3 (Fig. 9A), thus being probably reworked from unit K3 after that lake had dried
1219 up. Despite sedimentological differences, the palaeoecology of the lake was apparently
1220 very similar to that of K3, with the notable exception that remains of *Gerrothorax* are
1221 much rarer, albeit confined to articulated skeletons. This horizon also produced
1222 excellent skulls of *Mastodonsaurus*, which often include attached mandibles.
1223 Disarticulation of skulls does occur on a much smaller scale compared with that of unit
1224 K3. This indicates lower energy conditions in the lake K4 compared to K3, also
1225 allowing a much higher concentration of carbonate mud. This is consistent with the
1226 lower terrigenous (detrital) input in K4a compared to K3, exemplified by the drop in
1227 the abundance of quartz grains from K3 to K4.

1228 The tetrapods were mostly found at the top of the K4a unit, similar to the
1229 situation in K3 and the skull-bearing surface of E6c at Vellberg-Eschenau (Schoch and
1230 Seegis, 2016). In sum, these observations testify that very local and short-term droughts
1231 occurred, producing minor desiccation cracks, and probably locally restricted
1232 annihilation of the aquatic fauna. Predation dismembered the skeletons (Mujal et al.,
1233 2022) but there was not enough time to disarticulate skulls; these were concealed by
1234 the subsequent, fast sedimentation. Environmentally, and considering the similar
1235 ecosystems ecology, the K4a setting was probably not much different from the littoral

1236 zone preserved by K3, but with a different supply of sediment, both regarding the
1237 source and the rate of supply.

1238 The subsequently deposited layer K4b is slightly lighter, the generally more
1239 massive aspect and poor lamination suggests quieter conditions in the deposition. It
1240 must have formed under a calmer sedimentation regime than K4a, with equal amount
1241 of carbonate but less silt, and likely represents a slightly deeper lake facies. Like K4a,
1242 the pale brown mudstones of layer K4b are absent west of the Kupferzell excavation
1243 area, but they extend further N-NE, where they grade into darker grey mudstones that
1244 are also rich in fish scales.

1245 Finally, the sequence K4c appears to represent the return of a more coastal
1246 setting. The increasing frequency of *Darwinula* (Urlichs, pers. comm. 2021) suggests
1247 the dominance of freshwater conditions, which agrees with the tetrapod fauna,
1248 consisting of *Mastodonsaurus*, *Gerrothorax* and the 3 m long capitosaur *Kupferzellia*. The
1249 lack of juvenile *Mastodonsaurus* in layer K4c, which are very common in other lake
1250 deposits (Vellberg-Eschenau, Wolpertshausen, Michelbach an der Bilz), is remarkable.
1251 Whereas the presence of two large capitosaur predators indicates better living
1252 conditions (more abundant or diverse larger prey) than in the preceding lake phases,
1253 the occurrence of mostly large adult specimens of *Mastodonsaurus* forms a pattern
1254 consistent with ecological character displacement (Schluter and McPhail, 1992), with
1255 *Mastodonsaurus* and *Kupferzellia* separating more clearly in size to focus on different
1256 prey size. The frequency of *Batrachotomus* teeth and the occurrence of a *Nothosaurus*
1257 skeleton with bite traces of *Batrachotomus* (Mujal et al., 2022) are evidence of repeated
1258 drying and flooding, probably with water from different sources. The nothosaurid was
1259 probably washed in, or immigrated during a short-term connection with a lagoonal
1260 water body, possibly the large lagoon preserved in the Schwäbisch Hall-Gaildorf
1261 region.

1262 The marlstones of the layers K4a–c are locally more restricted than the unit K3.
1263 There is a clear topographic difference between these three layers: whereas layer K4a
1264 ended at the eastern margin of the excavation area and graded into a drift line (Urlichs,
1265 pers. comm. 2021), its western extension ends somewhere east of the highway bridge
1266 south of Bauersbach (where it is definitely absent), giving a range of 600–800 m only.
1267 To the north and northeast, layer K4a ends abruptly, but its southern extension

1268 remains unknown. This forms the smallest area among the K4 layers, and possibly
1269 represents a locally restricted carbonate mud somewhat remote from the littoral zone.
1270 To the west, it is replaced by green mudstones similar to the K3 sequence, which
1271 suggests that the littoral lake environment had persisted there for a longer time;
1272 following this line of evidence, the littoral zone of Lake K3–4 was probably aligned in
1273 the area between Übrigshausen, Westernach and Bauersbach.

1274 The resemblance of the yellow marlstones to the Anoplophora-Dolomite at
1275 Vellberg-Eschenau (Schoch and Seegis, 2016) is remarkable. Conceivably, layer K4a
1276 formed on a carbonate mudflat that fell dry episodically but was mostly covered by
1277 shallow freshwater. Characeans and ostracods were even more abundant than in unit
1278 K3, consistent with the higher carbonate content. As the fish and tetrapod faunas from
1279 units K3 and K4a are essentially identical, it is highly probable that the two facies
1280 formed in neighbouring environments of the same lake basin; the longer persistence
1281 of the green mudstone facies west of the Kupferzell lagerstätte agrees with this
1282 interpretation. Therefore, even if a stark drought period took place in the excavation
1283 area at the end of the deposition of unit K3, some relic water bodies probably persisted.

1284 Finally, temnospondyl bones with marks of low weathering (mostly stage 1)
1285 and abundant bite traces produced by ziphodont teeth also suggest that there were
1286 repeated phases when parts of the lake floor fell dry, enabling the archosaur
1287 *Batrachotomus* to scavenge on amphibian carcasses (Mujal et al., 2022). This scenario is
1288 supported by the presence of abundant detached *Batrachotomus* teeth whose pulpa is
1289 still filled with yellow-brown marlstones (in several cases also including fish scales).
1290 In other fossil assemblages with archosaurs and theropod dinosaurs, similar
1291 occurrences of teeth and partially preserved skeletons indicate relatively low-energy
1292 environments roamed by scavengers (Hungerbühler, 1998; Augustin et al., 2020).

1293 The abundance of polzbergiid fish (*Dipteronotus*, *Serrolepis*) remains suggests a
1294 structured habitat (e.g., charophyte meadows; see also discussion in Zhao et al., 2020
1295 and Liu et al., 2021), because these disk-shaped fishes were adapted to maneuver on a
1296 narrow range. In this sense, the setting provided sufficient food supply, possibly
1297 consisting of small arthropods. The relatively abundant fragments of very small
1298 actinistian bones and the low frequency of bigger ones suggest that the K4-Kupferzell
1299 setting was used as a nursery ground by these fishes. Similarly, the abundance of

1300 *Gerrothorax* remains (up to 80 individuals) indicates a stable population of this
1301 plagiosaur (Hellrung, 2003), further denoting a well-established ecosystem in a
1302 subaquatic setting.

1303 *Nothosaurus*, a sauropterygian reptile that inhabited near-coastal settings or
1304 even open marine environments (Klein et al., 2016), was present in the layer K4c (Wild,
1305 1980; Hinz et al., 2020). As mentioned by Hinz et al. (2020), this suggests a greater
1306 marine influence on the environments at Kupferzell than previously thought. We
1307 suggest that during time of deposition of the top sequence of the UGM unit, the
1308 Kupferzell area might have been located on the most proximal (inland) zone of a tidal
1309 flat, i.e., the supratidal region. In a sabkha setting there are usually long periods of
1310 desiccation, and these environments are only flooded by the sea during spring tides
1311 (Lasemi et al., 2012). Thus, the environment is similar or equivalent to a lacustrine
1312 system as herein discussed for the UGM in Kupferzell. Also, the yellow dolostones
1313 composing the Anoplophora-Dolomite (unit K5) display large moulds of gypsum
1314 nodules (also found in the Anthrakonitbank, the previous carbonate unit, see Hagdorn
1315 et al., 2015; Mujal and Schoch, 2020), and such structures in these facies are
1316 characteristic from sabkha settings (Lasemi et al., 2012). This points to a certain degree
1317 of salinity in the waters. In this sense, Bachmann (2002) related the precipitation of
1318 gypsum within carbonates to a high salinity at the top of the *Lingula*-Dolomit (an upper
1319 unit within the Lower Keuper: Fig. 1A). This further indicates a restricted marine
1320 environment, which in the case of the topmost part of the UGM and the base of the
1321 Anoplophora-Dolomite, would be a sabkha or sabkha-like setting.

1322 The unit K5 marks the end of the depositional history of the Kupferzell lake K4.
1323 Due to the presence of marine reptiles (see Schoch, 1999), these carbonates suggest
1324 marine conditions, representing a new transgression phase. Nevertheless, the presence
1325 of *Unionites brevis* (see Urlichs, 1982), a freshwater to brackish bivalve, indicates that
1326 in any case this was a mixed environment, still with terrestrial influence/input. This
1327 suggests a slightly different palaeoenvironmental setting than at Vellberg-Eschenau,
1328 where the base of these carbonates contains *Mastodonsaurus* and *Batrachotomus*, i.e., a
1329 more terrestrialised/continental setting. We interpret the base of the Anoplophora
1330 Dolomite in the northern Württemberg region as a very shallow-water, coastal setting,
1331 probably not unlike the tidal flats of K4, and possibly in continuity with them. In this

1332 model, some areas were under stronger influence of marine systems (Kupferzell)
1333 whereas others remained more protected from the open sea (Vellberg-Eschenau),
1334 possibly by some geographical barriers. In fact, the succession at Vellberg-Eschenau
1335 shows a transition to more terrestrial conditions from layers E4 to E6 at the top of the
1336 UGM (Schoch and Seegis, 2016), denoting fluctuations in the degree of salinity (likely
1337 correlated to marine influence) of the environments. Similarly, within and on top of
1338 layer E7a (base of the Anoplophora-Dolomite) in Vellberg-Eschenau *Batrachotomus*
1339 remains are particularly abundant (Schoch and Seegis, 2016).

1340

1341 7. Palaeoecology and ecosystem evolution

1342

1343 7.1. General features

1344

1345 The profound similarities between the contemporaneous vertebrate faunas of
1346 Kupferzell (Fig. 4) and Vellberg-Eschenau (Schoch and Seegis, 2016) and the
1347 lithological differences between the main fossiliferous layers prompt a more detailed
1348 comparison. Both deposits are interpreted as lacustrine, based on the presence of
1349 numerous non-marine taxa. On the other hand, there is some evidence of marine
1350 influence in both settings for certain periods (or seasons), as sporadic remains of
1351 sauropterygian carcasses (*Nothosaurus*) have been reported from both localities
1352 (Schoch and Seegis, 2016; Hinz et al., 2020). We have concluded above that these lakes
1353 developed in a sabkha-like setting, located on the most proximal part of a tidal flat that
1354 experienced frequent, and probably prolonged, periods of desiccation.

1355 The most fossiliferous layer at Vellberg-Eschenau (E6) is a deposit of dark grey,
1356 bedded claystones, very different from the silty and marly, light coloured deposits of
1357 Kupferzell (units K3 and K4). Despite these differences, both localities have a very
1358 similar faunal range (for comparison, see Schoch and Seegis, 2016). Thus, even though
1359 there are lateral changes in facies (see also Urlichs, 1982), the biotic components of the
1360 ecosystems were the same. Therefore, despite the existence of different, small-sized
1361 depocentres that built up independent lakes (especially in terms of sediment supply),
1362 there were no major physical barriers for the biota. In summary, this points to a well-
1363 stabilized, structured and diverse ecosystem yielding both aquatic dependant and

1364 terrestrial faunas. Both lagerstätten are characterised by the preponderance of bony
1365 fishes and temnospondyls, and the presence of a more terrestrial top predator,
1366 represented by the pseudosuchian *Batrachotomus* (see discussion in Mujal et al., 2022),
1367 is noteworthy.

1368 The high abundance of plagiosaurid remains in Kupferzell is remarkable,
1369 accounting for at least half of the tetrapod specimens. The dorsoventrally flattened
1370 *Gerrothorax* lived as a bottom-dweller in subaquatic environments, and its abundance
1371 indicates perennial water bodies. In any case, such lakes eventually underwent
1372 desiccation, which led to mass mortality events of the plagiosaurids and all the fishes
1373 in these ecosystems. The abundance of the large capitosaur *Mastodonsaurus*, which is
1374 considered by its sheer size the top predator in these lacustrine ecosystems, is a much
1375 more widespread feature shared with the deposits at Vellberg-Eschenau and many
1376 other localities in the region (Schoch and Seegis, 2016) as well as in Thuringia
1377 (Hagdorn et al., 2015).

1378 These lacustrine faunas sometimes contain taxa from terrestrial environments,
1379 such as parareptiles, small diapsids, archosauriforms and pseudosuchian archosaurs
1380 (Schoch, 2015). In addition, mud cracks and bone flaking indicate repeated subaerial
1381 exposure. Altogether, these features evidence a mixture of material from different
1382 environments, similar to the Grenzbonebed which contains faunas from both
1383 lacustrine and shallow marine habitats (Hagdorn et al., 2015). It is plausible that a
1384 substantial portion of the isolated bones that contribute to the bone clusters and
1385 accumulations in unit K3 was transported from the proper habitats of the preserved
1386 taxa. Prefossilisation, as indicated by the frequent amount and mode of bone
1387 fragmentation, confirms the allochthonous or parautochthonous state of some taxa,
1388 adding to the interpretation of a small-scale, patchy setting. However, at Kupferzell,
1389 most of the prefossilised bones stem from the same temnospondyl taxa as the
1390 skeletons, which suggests that the fragmentary bones were reworked from nearby
1391 deposits of the same or a very similar water body.

1392

1393 *7.2. Scenario of environmental and ecological evolution*

1394

1395 The reported observations can be compiled to create a detailed scenario for the
1396 fossiliferous sequence at Kupferzell (Fig. 13). After a long period in which coal-
1397 producing swamps had existed on a vast plain in the northern Württemberg region
1398 (K1), a minor sea level rise led to a short-term incursion of shallow marine water in the
1399 Kupferzell area (K2). Subsequent partial erosion produced m-wide channels on top of
1400 the K2 unit, followed by the deposition of silty claystones (K3) of lacustrine origin. The
1401 initial phase of this deposition was not particularly favourable for the settlement of
1402 ecosystems, as the low number of fossil remains in the first half of unit K3 suggests.

1403 Once fully established, this water body (Lake Kupferzell K3) harboured diverse
1404 freshwater fishes and the temnospondyls *Gerrothorax*, *Mastodonsaurus* and *Kupferzellia*.
1405 These formed the main predators in the lake, whereas the temnospondyls *Trematolestes*
1406 and *Plagiosuchus* probably lived in separate, but nearby water bodies, because their
1407 fragmentary bones were occasionally washed into the basin at the Kupferzell site,
1408 probably in periods of raised water levels. Remarkably, in Triassic fossil sites
1409 elsewhere (e.g., Sulej, 2002; Shishkin and Sulej, 2009; Lucas et al., 2010; Fortuny et al.,
1410 2011; Schoch, 2018), bone assemblages (including bone beds) of multiple individuals
1411 of a single taxon (with one or two additional taxa) are present. They differ from the
1412 condition observed in Kupferzell and other Lower Keuper localities, where multiple
1413 temnospondyl taxa coexisted; yet, only two taxa were dominant in Kupferzell
1414 (*Gerrothorax* and *Mastodonsaurus*). In this sense, the Lower Keuper lagerstätten (e.g.,
1415 Hagdorn et al., 2015; Schoch and Seegis, 2016; Schoch et al., 2018) may show that, in
1416 localities with lower faunal diversity, potential biases exist. These may be
1417 environmental and/or preservational in nature. In fact, this is also the case in the
1418 Triassic tetrapod footprint record (De Jaime-Soguero et al., 2021; Klein and Lucas,
1419 2021), with a conspicuous low number of temnospondyl footprints despite those were
1420 common components of the Triassic ecosystems as shown by the skeletal record. This
1421 is most probably due to an environmental bias against the preservation of
1422 temnospondyl ichnites (Mujal and Schoch, 2020).

1423 The chroniosuchian *Bystrowiella* probably dwelled more remote regions of
1424 rivers that occasionally washed its heavily worn skeletal remains into the locality. The
1425 lake shore was roamed by large archosaurs (*Batrachotomus*) looking for prey and
1426 carcasses (Mujal et al., 2022). An ostracod-rich, marly sediment enriched with

1427 vertebrate skeletal elements accumulated at the lake bottom. Periodically, enhanced
1428 levels of precipitation led to the increase of rivers, eroding parts of the lake shores and
1429 taking large amounts of unconsolidated lake sediments, incorporating vertebrate
1430 remains and carcasses in the sedimentary matrix (cf. Fig. 12A). This was the source for
1431 the large amount of reworked, prefossilised bones in the unit K3 of the lagerstätte. In
1432 one or more such events, water flowed as flash floods to the west where it oozed away
1433 on the mudplain, filling up the mud cracks with fossiliferous marl and repeatedly
1434 leaving a marly blanket with vertebrate bones and occasional carcasses behind. As
1435 shown by the large mud cracks on top of K3 (Fig. 7A), the plain lay dry for a long
1436 period marking the end of the depositional cycle of the lake. Individuals of
1437 *Batrachotomus* roamed on the remaining dry plain, feeding on carcasses of
1438 *Mastodonsaurus* and even conspecifics (Mujal et al., 2022) that had died by catastrophic
1439 inundations or by droughts. Of note, as in other Triassic localities (Hungerbühler,
1440 1998; França et al., 2011; Nesbitt et al., 2020), different individuals of pseudosuchians
1441 have been found together, suggesting a hypothetical gregarious behaviour in the
1442 group (Nesbitt et al., 2020). In fact, considering the direct evidence of interaction in
1443 *Batrachotomus* such social behaviour is plausible (Mujal et al., 2022).

1444 The plain was subsequently covered by a perennial freshwater body, here
1445 referred to as Lake Kupferzell K4. The conditions apparently became favourable
1446 sooner than during the evolution of Lake Kupferzell K3, permitting a faster settlement
1447 of freshwater dwellers and the build-up of a lake ecosystem. The lake floor consisted
1448 of calcareous marly sediments (layer K4a), and charophyte meadows and ostracods
1449 were more abundant than in Lake K3. The fish fauna was somewhat less diverse than
1450 that of Lake K3, and *Gerrothorax* was less frequent than *Mastodonsaurus*. Like in Lake
1451 K3, the caiman-like capitosaur *Kupferzellia* was also present, suggesting that this new
1452 water body was equally rich in nutrients than the former. Sedimentation was fast
1453 enough that *Gerrothorax* skeletons could be preserved in articulation or with skeletal
1454 elements scattered over a small area only (Hellrung, 2003; Fig. 12B). However, the lack
1455 of articulated fish skeletons and absence of sedimentary lamination point to an active
1456 organic life at the oxygenated lake bottom.

1457 After the first phase of Lake K4, the basin fell dry and was subsequently filled
1458 with flow deposits and partially reworked sediments (horizon K4a). Then, a deeper

1459 water table with calmer energy conditions was established, characterised by carbonate
1460 muds and less abundant ostracods and charophytes (horizon K4b). In the final phase
1461 of Lake K4, light-brown, finely laminated marlstones (horizon K4c) were deposited,
1462 indicating a shallower third and final phase of the lake. In K4c, quartz grains are much
1463 more abundant than in K4b, and the presence of lamination suggests increased water
1464 currents.

1465 The concentration of skulls of *Mastodonsaurus* and *Kupferzellia* at the top of the
1466 K4 sequence suggests a further event of shallowing with an eventual desiccation of the
1467 lake with mass mortality among the fishes and temnospondyls. Widespread
1468 disarticulation of skeletons was probably caused by water currents. This horizon is
1469 similar to the top of E6d at Vellberg-Eschenau in sedimentary features as well as the
1470 accumulation of temnospondyl skulls (Schoch and Seegis, 2016). A similar taphonomic
1471 sequence has been inferred for other temnospondyl bone assemblages (Lucas et al.,
1472 2010).

1473 At Kupferzell, the overlying Anoplophora-Dolomite (K5) were probably
1474 deposited on a carbonate mud plain. The facies at Kupferzell is consistent with the
1475 lithologically very similar and stratigraphically equivalent unit E7 at the Vellberg-
1476 Eschenau site (Schoch and Seegis, 2016). Except for sporadic bone remains (Kupferzell)
1477 or rare *Batrachotomus* and *Mastodonsaurus* skeletons (Vellberg-Eschenau), fossils are
1478 absent in these coastal dolostones; this environment was probably hostile to most
1479 invertebrates, with extremely shallow salty water that frequently dried out
1480 completely.

1481

1482 **8. Conclusions**

1483

1484 Our analysis of the Middle Triassic Kupferzell fossil lagerstätte revealed two
1485 successive lakes that harboured similar ecosystems. These were dominated by
1486 freshwater fishes and temnospondyl apex predators, with occasional incursions of
1487 terrestrial archosaurs in the littoral zone. The larger environment, a carbonate
1488 mudplain with coexisting large brackish lagoons (10–20 km) and small freshwater
1489 lakes (5–10 km), covered a vast area including the generally similar fossil lagerstätte of
1490 Vellberg-Eschenau and others in the vicinity. The lagoons appear to have been

1491 relatively long-lived and stable, whereas the lakes fluctuated on a shorter time scale
1492 with repeated periods of partial droughts.

1493 The studied lake systems built on top of more widespread and uniform marine-
1494 lagoonal sequences, and probably document a progressing shallowing and eventual
1495 closure of the basin. The formation of the small lakes allowed the establishment of rich
1496 ecosystems, including aquatic and riparian organisms, and encompassing taxa that
1497 tolerated saline waters. The Kupferzell fossil lagerstätte preserves the evolution of two
1498 clearly differentiated lakes, separated by an intense drought period. This fits well in a
1499 sabkha setting, a proximal supratidal flat with only occasional marine influence.

1500 The exceptional Kupferzell fossil lagerstätte was not only taxonomically
1501 diverse, but also rich in taphonomic features, permitting the reconstruction of
1502 palaeoecological traits of some taxa (e.g., Mujal et al., 2022). By their richness and
1503 quality of preservation, the Kupferzell and Vellberg-Eschenau deposits rank among
1504 the best known Middle Triassic vertebrate deposits. The faunal richness in both
1505 abundance and diversity of the Lower Keuper suggests that potential environmental
1506 and/or preservational biases (rather than impoverished ecosystems) exist in other
1507 Triassic localities. Several trophic levels are identified, including different apex
1508 predators. They preserve a rich, complex and well-structured ecosystem, despite the
1509 frequent occurrence of droughts that often reshaped the environmental settings.

1510 Future work on these Triassic lake deposits may study (1) the wider geographic
1511 distribution and topographical diversity of these depositional basins, (2) the ecological
1512 diversity and distinctness between lakes, and (3) the evolution of complex ecosystems
1513 and trophic webs during the Triassic, in the rise and dominance of the archosaur
1514 lineage. Considering its vast outcrop area, the excellent study conditions and the
1515 quantity of as yet unstudied fossil lagerstätten, the Central European Basin will
1516 continue to provide case studies for these topics.

1517

1518 **Acknowledgements**

1519 We thank Rupert Wild, Max Urlichs and Ronald Böttcher (SMNS) for sharing many
1520 first-hand observations with us. Our SMNS preparation crew, especially Norbert
1521 Adorf and Isabell Rosin, along with many additional supporters and private collectors,
1522 are thanked for their continued efforts in planning, organising and conducting field

1523 work; their enormous enthusiasm made this project possible. Christoph Wimmer-Pfeil
1524 (SMNS) skilfully prepared the thin sections. Werner Kugler, Frank Ullmann, Brigitte
1525 Rozynek, Traugott and Ute Haubold, and Hans Michael Salomon contributed in many
1526 ways to the current project. Hans Hagdorn (Muschelkalkmuseum, Ingelfingen) is
1527 thanked for access to specimens and much support over three decades. Erin Maxwell
1528 (SMNS), Edgar Nitsch (Geologisches Landesamt Freiburg) and Theo Simon
1529 (Fichtenberg) helped with many discussions. We thank the comments and suggestions
1530 of an anonymous reviewer and Spencer G. Lucas, as well as the editor Prof. Lucia
1531 Angiolini, who helped to improve a previous version of the manuscript.

1532

1533 **References**

1534

- 1535 Agassiz, L. 1833–1843. *Recherches sur les poissons fossiles*. 5 volumes, Neuchâtel.
- 1536 Alonso-Zarza, A.M., Wright, V.P. 2010. Palustrine carbonates. In: Alonso-Zarza, A.M.,
1537 Tanner, L.H. (Eds.), *Carbonates in continental settings. Developments in*
1538 *Sedimentology*, 61, pp. 103–131.
- 1539 Augustin, F.J., Matzke, A.T., Maisch, M.W., Pfretzeschner, H.-U. 2020. A theropod
1540 dinosaur feeding site from the Upper Jurassic of the Junggar Basin, NW China.
1541 *Palaeogeography, Palaeoclimatology, Palaeoecology* 560, 109999.
- 1542 Bachmann, G.H. 2002. A Lamellibranch-Stromatolite Bioherm in the Lower Keuper
1543 (Ladinian, Middle Triassic), South Germany. *Facies* 46, 83–88.
- 1544 Beutler, G., Gründel, J. 1963. Die Ostracoden des Unteren Keupers im Bereich des
1545 Thüringer Beckens. *Freiberger Forschungshefte C164*, 33–92.
- 1546 Beutler, G., Hauschke, N., Nitsch, E. 1999. Faziesentwicklung des Keupers im
1547 Germanischen Becken. In: Hauschke, N., Wilde, V. (Eds.), *Trias. Eine ganz andere*
1548 *Welt*. Dr. Friedrich Pfeil, München, pp. 129–174.
- 1549 Behrensmeier, A.K. 1978.
1550 Taphonomic and ecologic information from bone weathering. *Paleobiology* 4, 150–
162.
- 1551 Behrensmeier, A.K., Hook, R.W. 1992. Paleoenvironmental contexts and taphonomic
1552 modes. In: Behrensmeier, A.K., Damuth, J.D., DiMichele, W.A., Potts, R., Sues, H.-
1553 D., Wing, S.L. (Eds.), *Terrestrial ecosystems through time*. University of Chicago
1554 Press, Chicago, pp. 15–136.

- 1555 Binford, L.R. 1981. *Bones: ancient men and modern myths*. 1st edition. Academic Press,
1556 London, 320 pp.
- 1557 Böttcher, R. 2015. Fische des Lettenkeupers. In: Hagdorn, H., Schoch, R.R., Schweigert,
1558 G. (Eds.), *Der Lettenkeuper – Ein Fenster in die Zeit vor den Dinosauriern*.
1559 *Palaeodiversity Sonderband 2015*, pp. 141–202.
- 1560 Britt, B.B., Eberth, D.A., Scheetz, R.D., Greenhalgh, B.W., Stadtman, K.L. 2009.
1561 *Taphonomy of debris-flow hosted dinosaur bonebeds at Dalton Wells, Utah*
1562 *(Lower Cretaceous, Cedar Mountain Formation, USA)*. *Palaeogeography,*
1563 *Palaeoclimatology, Palaeoecology* 280, 1–22.
- 1564 Brodie, P.B. 1843. *A History of the Fossil Insects in the Secondary Rocks of England*:
1565 London, John Van Voorst, 130 p.
- 1566 Brunner, H. 1973. *Stratigraphische und sedimentpetrographische Untersuchungen am*
1567 *Unteren Keuper (Lettenkeuper, Trias) im nördlichen Baden-Württemberg.*
1568 *Arbeiten aus dem Institut für Geologie und Paläontologie der Universität Stuttgart*
1569 *N.F. 70*, 1–85.
- 1570 Brunner, H. 1977. *Zur Stratigraphie und Sedimentpetrographie des Unteren Keupers*
1571 *(Lettenkeuper, Trias) im nördlichen Baden-Württemberg*. *Jahresberichte und*
1572 *Mitteilungen des Oberrheinischen Geologischen Vereins* 59, 169–193.
- 1573 Brunner, H. 1980. *Zur Stratigraphie des Unteren Keupers (Lettenkeuper, Trias) im*
1574 *nordwestlichen Baden-Württemberg*. *Jahresberichte und Mitteilungen des*
1575 *Oberrheinischen Geologischen Vereins* 62, 207–216.
- 1576 Brunner, H., Bruder, J. 1977. *Standardprofile des Unteren Keupers (Lettenkeuper,*
1577 *Trias) im nördlichen Baden-Württemberg*. *Jahresberichte und Mitteilungen des*
1578 *Oberrheinischen Geologischen Vereins* 63, 253–269.
- 1579 Chen, Z.-Q., Benton, M.J. 2012. *The timing and pattern of biotic recovery following the*
1580 *end-Permian mass extinction*. *Nature Geosciences* 5, 375–383.
- 1581 Cohen, A.S., Thouin, C. 1987. *Nearshore carbonate deposits in Lake Tanganyika.*
1582 *Geology* 15, 414–418.
- 1583 Dames, W. 1888. *Die Ganoiden des deutschen Muschelkalks*. *Paläontologische*
1584 *Abhandlungen* 4 (2), 133–180.

- 1585 D'Amore, D.C., Blumenschine, R.J. 2009. Komodo monitor (*Varanus komodoensis*)
1586 feeding behavior and dental function reflected through tooth marks on bone
1587 surfaces, and the application to ziphodont paleobiology. *Paleobiology* 35, 525–552.
- 1588 D'Amore, D.C., Blumenschine, R.J. 2012. Using striated tooth marks on bone to predict
1589 body size in theropod dinosaurs: a model based on feeding observations of
1590 *Varanus komodoensis*, the Komodo monitor. *Paleobiology* 38, 79–100.
- 1591 De Jaime-Soguero, C., Mujal, E., Dinarès-Turell, J., Oms, O., Bolet, A., Orlandi-
1592 Oliveras, G., Fortuny, J. 2021. Palaeoecology of Middle Triassic tetrapod
1593 ichnoassociations (middle Muschelkalk, NE Iberian Peninsula) and their
1594 implications for palaeobiogeography in the western Tethys region.
1595 *Palaeogeography, Palaeoclimatology Palaeoecology* 565, 110204.
- 1596 Dorka, M. 2001. Shark remains from the Triassic of Schöningen, Lower Saxony,
1597 Germany. *Neues Jahrbuch für Geologie und Paläontologie* 221, 219–247.
- 1598 Drumheller, S.K., McHugh, J.B., Kane, M., Riedel, A., D'Amore, D.C. 2020. High
1599 frequencies of theropod bite marks provide evidence for feeding, scavenging, and
1600 possible cannibalism in a stressed Late Jurassic ecosystem. *PLoS One* 15, e0233115.
- 1601 Etzold, A., Schweizer, V. 2005. Der Keuper in Baden-Württemberg. In: Deutsche
1602 Stratigraphische Kommission (Eds.), *Stratigraphie von Deutschland IV. Keuper*.
1603 Bearbeitet von der Arbeitsgruppe Keuper der Subkommission Perm-Trias der
1604 DSK. *Courier Forsch. Senckenberg* 253, 215–258.
- 1605 Fiorillo, A.R. 1988. Taphonomy of Hazard Homestead Quarry (Ogallala Group),
1606 Hitchcock County, Nebraska. *Contributions to Geology, University of Wyoming*
1607 26, 57–97.
- 1608 Fortuny, J., Galobart, À., De Santisteban, C. 2011. A new capitosaur from the Middle
1609 Triassic of Spain and the relationships within the Capitosauria. *Acta*
1610 *Palaeontologica Polonica* 56 (3), 553–566.
- 1611 Fraas, E. 1896. Die schwäbischen Trias-Saurier nach dem Material der Kgl. Naturalien-
1612 Sammlung in Stuttgart zusammengestellt. Stuttgart: E. Schweizerbart'sche
1613 Verlagshandlung.
- 1614 França, M.A.G., Ferigolo, J., Langer, M.C. 2011. Associated skeletons of a new Middle
1615 Triassic “Rauisuchia” from Brazil. *Naturwissenschaften* 98, 389–395.

- 1616 Franz, M., Henniger, M., Barnasch, J. 2013. The strong diachronous
1617 Muschelkalk/Keuper facies shift in the Central European Basin: implications from
1618 the type-section of the Erfurt Formation (Lower Keuper, Triassic) and basin-wide
1619 correlations. *International Journal of Earth Sciences (Geologische Rundschau)* 102,
1620 761–780.
- 1621 Franz, M., Nowak, K., Berner, U., Heunisch, C., Bandel, K., Röhling, H.-G.,
1622 Wolfgramm, M. 2014. Eustatic control on epicontinental basins: The example of
1623 the Stuttgart Formation in the Central European Basin (Middle Keuper, Late
1624 Triassic). *Global and Planetary Change* 122, 305–329.
- 1625 Franz, M., Kaiser, S.I., Fischer, J., Heunisch, C., Kustatscher, E., Luppold, F.W., Berner,
1626 U., Röhling, H.-G. 2015. Eustatic and climatic control on the Upper Muschelkalk
1627 Sea (late Anisian/Ladinian) in the Central European Basin. *Global Planetary
1628 Change* 135, 1–27.
- 1629 Frey, E., Monninger, S. 2010. Lost in action—the isolated crocodylian teeth from Enspel
1630 and their interpretive value. *Palaeobiodiversity and Palaeoenvironments* 90, 65–
1631 81.
- 1632 Freytet, P., Plaziat, J.-C. 1982. Continental carbonate sedimentation and pedogenesis,
1633 Late Cretaceous and early Tertiary of southern France. *Contributions to
1634 Sedimentology* 12, 213 p.
- 1635 Freytet, P., Verrecchia, E.P. 2002. Lacustrine and palustrine carbonate petrography: an
1636 overview. *Journal of Paleolimnology* 27, 221–237.
- 1637 Geyer, G., Hautmann, M., Hagdorn, H., Ockert, W., Streng, M. 2005. Well-preserved
1638 mollusks from the Lower Keuper (Ladinian) of Hohenlohe (Southwest Germany).
1639 *Paläontologische Zeitschrift* 79, 429–460.
- 1640 Goehring, L. 2013. Evolving fracture patterns: columnar joints, mud cracks and
1641 polygonal terrain. *Philosophical Transactions of the Royal Society A* 371, 20120353.
- 1642 Goehring, L., Conroy, R., Akhter, A., Clegg, W.J., Routh, A.F. 2010. Evolution of mud-
1643 crack patterns during repeated drying cycles. *Soft Matter* 6, 3562–3567.
- 1644 Gordon, C.M., Roach, B.T., Parker, W.G., Briggs, D.E.G. 2020. Distinguishing
1645 regurgitalites and coprolite: a case study using a Triassic bromalite with soft tissue
1646 of the pseudosuchian archosaur *Revueltosaurus*. *Palaios* 35, 111–121.

- 1647 Gower, D.J. 1999. Cranial osteology of a new rauisuchian archosaur from the Middle
1648 Triassic of southern Germany. *Stuttgarter Beiträge zur Naturkunde B* 280, 1–49.
- 1649 Gower, D.J., Schoch, R.R. 2009. The postcranial skeleton of the rauisuchian
1650 *Batrachotomus kupferzellensis*. *Journal of Vertebrate Paleontology* 29, 103–122.
- 1651 Hagdorn, H., Schoch, R.R., Seegis, D., Werneburg, R. 2015. Wirbeltierlagerstätten im
1652 Lettenkeuper. In: Hagdorn, H., Schoch, R.R., Schweigert, G. (Eds), *Der*
1653 *Lettenkeuper – Ein Fenster in die Zeit vor den Dinosauriern*. *Palaeodiversity*
1654 *Sonderband* 2015, pp. 325–358.
- 1655 Hagdorn, H., Freudenberger, W., Röhling, H.-G., Röhling, S., Simon, T. 2021. Heutige
1656 Verbreitung des Muschelkalks und Abgrenzung der Bearbeitungsgebiete.
1657 *Schriftenreihe der Deutschen Gesellschaft für Geowissenschaften* 91, 33–40.
- 1658 Haynes, G. 1983. Frequencies of spiral and green-bone fractures on ungulate limb
1659 bones in modern surface assemblages: *American Antiquity* 48, 102–114.
- 1660 Haynes, G., Krasinski, K., Wojtal, P. 2020. Elephant bone breakage and surface marks
1661 made by trampling elephants: Implications for interpretations of marked and
1662 broken *Mammuthus* spp. bones. *Journal of Archaeological Science: Reports* 33,
1663 102491.
- 1664 Haynes, G., Krasinski, K., Wojtal, P. 2021. A study of fractured proboscidean bones in
1665 recent and fossil assemblages. *Journal of Archaeological Method and Theory* 28,
1666 956–1025.
- 1667 Hellrung, H. 2003. *Gerrothorax pustuloglomeratus*, ein Temnospondyle (Amphibia) mit
1668 knöcherner Branchialkammer aus dem Unteren Keuper von Kupferzell
1669 (Süddeutschland). *Stuttgarter Beiträge zur Naturkunde B* 330, 1–130.
- 1670 Hinz, J.K., Matzke, A.T., Augustin, F.J., Pfretzschner, H.-U. 2020. A *Nothosaurus*
1671 (Sauropterygia) skull from Kupferzell (Triassic, late Ladinian; SW Germany).
1672 *Neues Jahrbuch für Geologie und Paläontologie* 297(1), 101–111.
- 1673 Hugli, J., Scheyer, T.M. 2012. Ossification sequences and associated ontogenetic
1674 changes in the bone histology of pachypleurosaurids from Monte San Giorgio
1675 (Switzerland/Italy). *Journal of Vertebrate Paleontology* 32 (2), 315–327.
- 1676 Hungerbühler, A. 1998. Taphonomy of the prosauropod dinosaur *Sellosaurus*, and its
1677 implications for carnivore faunas and feeding habits in the Late Triassic.
1678 *Palaeogeography, Palaeoclimatology, Palaeoecology* 143, 1–29.

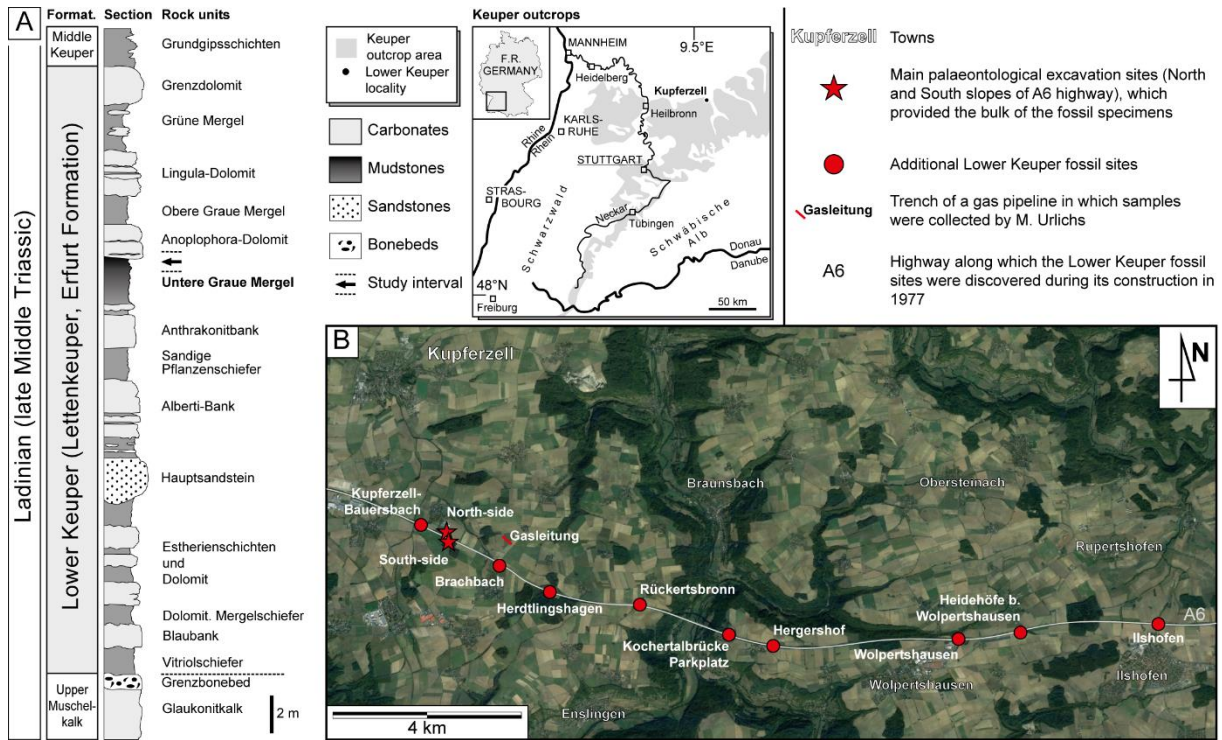
- 1679 Hunt, A.P., Lucas, S.G. 2021. The ichnology of vertebrate consumption: dentalites,
1680 gastroliths and bromalites. *New Mexico Museum Natural History Science Bulletin*
1681 87, 1–216.
- 1682 Irmis, R.B., Whiteside, J.H. 2012. Delayed recovery of non-marine tetrapods after the
1683 end-Permian mass extinction tracks global carbon cycle. *Proceedings of the Royal*
1684 *Society B* 279, 1310–1318.
- 1685 Jacobsen, A.R., Bromley, R.G. 2009. New ichnotaxa based on tooth impressions on
1686 dinosaur and whale bones. *Geological Quarterly* 53, 373–382.
- 1687 Jaeger, G.F. 1828. Über die fossile [sic] Reptilien, welche in Württemberg aufgefunden
1688 worden sind. J. B. Metzler, Stuttgart, 48 p.
- 1689 Klein, H., Lucas, S.G. 2021. The Triassic tetrapod footprint record. *New Mexico*
1690 *Museum Natural History Science Bulletin* 83, 1–194.
- 1691 Klein, N., Sander, P.M., Krahl, A., Scheyer, T.M., Houssaye, A. 2016. Diverse aquatic
1692 adaptations in *Nothosaurus* spp. (Sauropterygia) – inferences from humeral
1693 histology and microanatomy. *PLoS One* 11, e0158448.
- 1694 Lasemi, Y., Jahani, D., Amin-Rasouli, H., Lasemi, Z. 2012. Ancient carbonate tidalites.
1695 In: Davis, Jr., R.A., Dalrymple, R.W. (Eds.), *Principles of Tidal Sedimentology*.
1696 Springer, pp. 567–607.
- 1697 Liu, H., Qiu, Z., Zou, C., Fu, J., Zhang, W., Tao, H., Li, S., Zhou, S., Wang, L., Chen, Z.-
1698 Q. 2021. Environmental changes in the Middle Triassic lacustrine basin (Ordos,
1699 North China): Implication for biotic recovery of freshwater ecosystem following
1700 the Permian-Triassic mass extinction. *Global and Planetary Change* 204, 103559.
- 1701 Lucas, S.G. 2017. Permian tetrapod extinction events. *Earth-Science Reviews* 170, 31–
1702 60.
- 1703 Lucas, S.G. 2021. Nonmarine mass extinctions. *Paleontological Research* 25, 329–344.
- 1704 Lucas, S.G., Rinehart, L.F., Krainer, K., Spielmann, J.A., Heckert, A.B. 2010.
1705 Taphonomy of the Lamy amphibian quarry: A Late Triassic bonebed in New
1706 Mexico, U.S.A. *Palaeogeography, Palaeoclimatology, Palaeoecology* 298, 388–398.
- 1707 Mikuláš, R., Kadlecová, E., Fejfar, O., Dvořák, Z. 2006. Three new ichnogenera of biting
1708 and gnawing traces on reptilian and mammalian bones: a case study from the
1709 Miocene of the Czech Republic. *Ichnos* 13, 113–127.

- 1710 Mujal, E., Schoch, R.R. 2020. Middle Triassic (Ladinian) amphibian tracks from the
1711 Lower Keuper succession of southern Germany: Implications for temnospondyl
1712 locomotion and track preservation. *Palaeogeography, Palaeoclimatology*
1713 *Palaeoecology* 543, 109625.
- 1714 Mujal, E., Foth, C., Maxwell, E.E., Seegis, D., Schoch, R.R. 2022. Feeding habits of the
1715 Middle Triassic pseudosuchian *Batrachotomus kupferzellensis* from Germany and
1716 palaeoecological implications for archosaurs. *Palaeontology* 65 (3), e12597.
- 1717 Nesbitt, S.J., Zawiskie, J.M., Dawley, R.M. 2020. The osteology and phylogenetic
1718 position of the loricatan (Archosauria: Pseudosuchia) *Heptasuchus clarki*, from the
1719 ?Mid-Upper Triassic, southeastern Big Horn Mountains, Central Wyoming (USA).
1720 *PeerJ* 8, e10101.
- 1721 Nitsch, E. 2003. Wie kommt das Salz in den Keuper? *Beiträge zur Geologie von*
1722 *Thüringen* 10, 75–110.
- 1723 Nitsch, E. 2015. Fazies und Ablagerungsräume. In: Hagdorn, H., Schoch, R.R.,
1724 Schweigert, G. (Eds.), *Der Lettenkeuper – Ein Fenster in die Zeit vor den*
1725 *Dinosauriern*. *Palaeodiversity Sonderband 2015*, pp. 285-324.
- 1726 Njau, J., Blumenshine, R.J. 2006. A diagnosis of crocodile feeding traces on larger
1727 mammal bone, with fossil examples from the Plio-Pleistocene Olduvai Basin,
1728 Tanzania. *Journal of Human Evolution* 50, 142–162.
- 1729 Njau, J., Gilbert, H.G. 2016. A taxonomy for crocodile-induced bone modifications and
1730 their relevance to paleoanthropology. *FOROST Occasional Publications* 3, 1–13.
- 1731 Pawlak, W., Rozwalak, P., Sulej, T. 2022. Triassic fish faunas from Miedary (Upper
1732 Silesia, Poland) and their implications for understanding paleosalinity.
1733 *Palaeogeography, Palaeoclimatology, Palaeoecology* 590, 110860.
- 1734 Pöppelreiter, M. 1999. Controls on epeiric successions exemplified with the mixed
1735 siliciclastic–carbonate Lower Keuper (Ladinian, German Basin). *Tübinger*
1736 *Geowissenschaftliche Arbeiten A* 51, 1–126.
- 1737 Pöppelreiter, M., Aigner, T. 2003. Unconventional pattern of reservoir facies
1738 distribution in epeiric successions: Lessons from an outcrop analog (Lower
1739 Keuper, Germany). *AAPG Bulletin* 87(1), 39–70.
- 1740 Pöppelreiter, M., Aigner, T. 2008. High-resolution sequence stratigraphy, facies
1741 patterns and controls in a mixed epeiric shelf: implications for reservoir prediction

- 1742 (Lower Keuper, Triassic, German Basin). Geological Association of Canada Special
1743 Paper 48, 283–301.
- 1744 Pratt, B.R. 1998. Syneresis cracks: subaqueous shrinkage in argillaceous sediments
1745 caused by earthquake-induced dewatering. *Sedimentary Geology* 117, 1–10.
- 1746 Quenstedt, F.A., 1880. Begleitworte zur Geognostischen Specialkarte von
1747 Württemberg, Atlasblatt Hall. Stuttgart.
- 1748 Romano, M., Bernardi, M., Petti, F.M., Rubidge, B., Hancox, J., Benton, M.J., 2020. Early
1749 Triassic terrestrial tetrapod fauna: a review. *Earth-Science Reviews* 210, 103331.
- 1750 Ryan, M.J., Russell, A.P., Eberth, D.A., Currie, P.J. 2001. The taphonomy of a
1751 *Centrosaurus* (Ornithischia: Certopsidae) Bone Bed from the Dinosaur Park
1752 Formation (Upper Campanian), Alberta, Canada, with comments on cranial
1753 ontogeny. *Palaios* 16, 482–506.
- 1754 Sanchez, S., Schoch, R.R. 2013. Bone histology reveals a high environmental and
1755 metabolic plasticity as a successful evolutionary strategy in a long-lived
1756 homeostatic Triassic temnospondyl. *Evolutionary Biology* 40, 627–647.
- 1757 Seebach, K. v. 1857. Entomotraken aus der Trias Thüringens. *Zeitschrift der*
1758 *Deutschen Geologischen Gesellschaft* 9, 198–206.
- 1759 Schluter, D., McPhail, J.D. 1992. Ecological character displacement and speciation in
1760 sticklebacks. *The American Naturalist* 140, 85–108.
- 1761 Schmid, E.E. 1861. Die Fischzähne der Trias bei Jena. *Nova Acta Academiae Caesareae*
1762 *Leopoldino-Carolinae Germanicae Naturae Curiosorum* 29 (9), 42 p.
- 1763 Schoch, R.R. 1997. A new capitosaur amphibian from the Upper Lettenkeuper
1764 (Triassic: Ladinian) of Kupferzell (Southern Germany). *Neues Jahrbuch für*
1765 *Geologie und Paläontologie* 203, 239–272.
- 1766 Schoch, R.R. 1999. Comparative osteology of *Mastodonsaurus giganteus* (Jaeger, 1828)
1767 from the Middle Triassic (Lettenkeuper: Longobardian) of Germany (Baden-
1768 Württemberg, Bayern, Thüringen). *Stuttgarter Beiträge zur Naturkunde B* 278, 1–
1769 175.
- 1770 Schoch, R.R. 2002. Stratigraphie und Taphonomie wirbeltierreicher Schichten im
1771 Unterkeuper (Mitteltrias) von Vellberg (SW-Deutschland). *Stuttgarter Beiträge zur*
1772 *Naturkunde B* 318, 1–30.

- 1773 Schoch, R.R. 2006. A complete trmatosaurid amphibian from the Middle Triassic of
1774 Germany. *Journal of vertebrate Paleontology* 26 (1), 29–43.
- 1775 Schoch, R.R. 2018. The temnospondyl *Parotosuchus nasutus* (v. Meyer, 1858) from the
1776 Early Triassic Middle Buntsandstein of Germany. *Palaeodiversity* 11, 107–126.
- 1777 Schoch, R.R., Seegis, D. 2016. A Middle Triassic palaeontological gold mine: The
1778 vertebrate deposits of Vellberg (Germany). *Palaeogeography, Palaeoclimatology,*
1779 *Palaeoecology* 459, 249–267.
- 1780 Schoch, R.R., Sues, H.-D. 2014. A new archosauriform reptile from the Middle Triassic
1781 (Ladinian) of Germany. *Journal of Systematic Palaeontology* 12(1), 113–131.
- 1782 Schoch, R.R., Ullmann, F., Rozynek, B., Ziegler, R., Seegis, D., Sues, H.-D. 2018.
1783 Tetrapod diversity and palaeoecology in the German Middle Triassic (Lower
1784 Keuper) documented by tooth morphotypes. *Palaeobiodiversity and*
1785 *Palaeoenvironments* 98, 615–638.
- 1786 Schoch, R.R., Witzmann, F., 2011. Cranial morphology of the plagiosaurid *Gerrothorax*
1787 *pulcherrimus* as an extreme example of evolutionary stasis. *Lethaia* 45, 371–385.
- 1788 Schultze, H.-P. 1981. Das Schädeldach eines ceratodontiden Lungenfisches aus der
1789 Trias Süddeutschlands (Dipnoi, Pisces). *Stuttgarter Beiträge Naturkunde B* 70, 1–
1790 31.
- 1791 Shishkin, M.A. Sulej, T. 2009. The Early Triassic temnospondyls of the Czatkowice 1
1792 tetrapod assemblage. *Palaeontologia Polonica* 65, 31–77.
- 1793 Sues, H.-D., Fraser, N.C. 2010. *Triassic Life on Land: The Great Transition*. Columbia
1794 University Press, New York, 236 p.
- 1795 Sues, H.-D., Schoch, R.R., Sobral, G., Irmis, R.B. 2020. A new archosauriform reptile
1796 with distinctive teeth from the Middle Triassic (Ladinian) of Germany. *Journal of*
1797 *Vertebrate Paleontology* 40 (1), e1764968.
- 1798 Sulej, T. 2002. Species discrimination of the Late Triassic temnospondyl amphibian
1799 *Metoposaurus diagnosticus*. *Acta Palaeontologica Polonica* 47 (3), 535–546.
- 1800 Sun, Y.D., Joachimski, M.M., Wignall, P.B., Yan, C.B., Chen, Y.L., Jiang, H.S., Wang,
1801 L.D., Lai, X.L. 2012. Lethally hot temperatures during the early Triassic
1802 Greenhouse. *Science* 338, 366–370.
- 1803 Tabor, N.J., Montañez, I.P., Scotese, C.R., Poulsen, C.J., Mack, G.H. 2008. Paleosol
1804 archives of environmental and climatic history in paleotropical Western

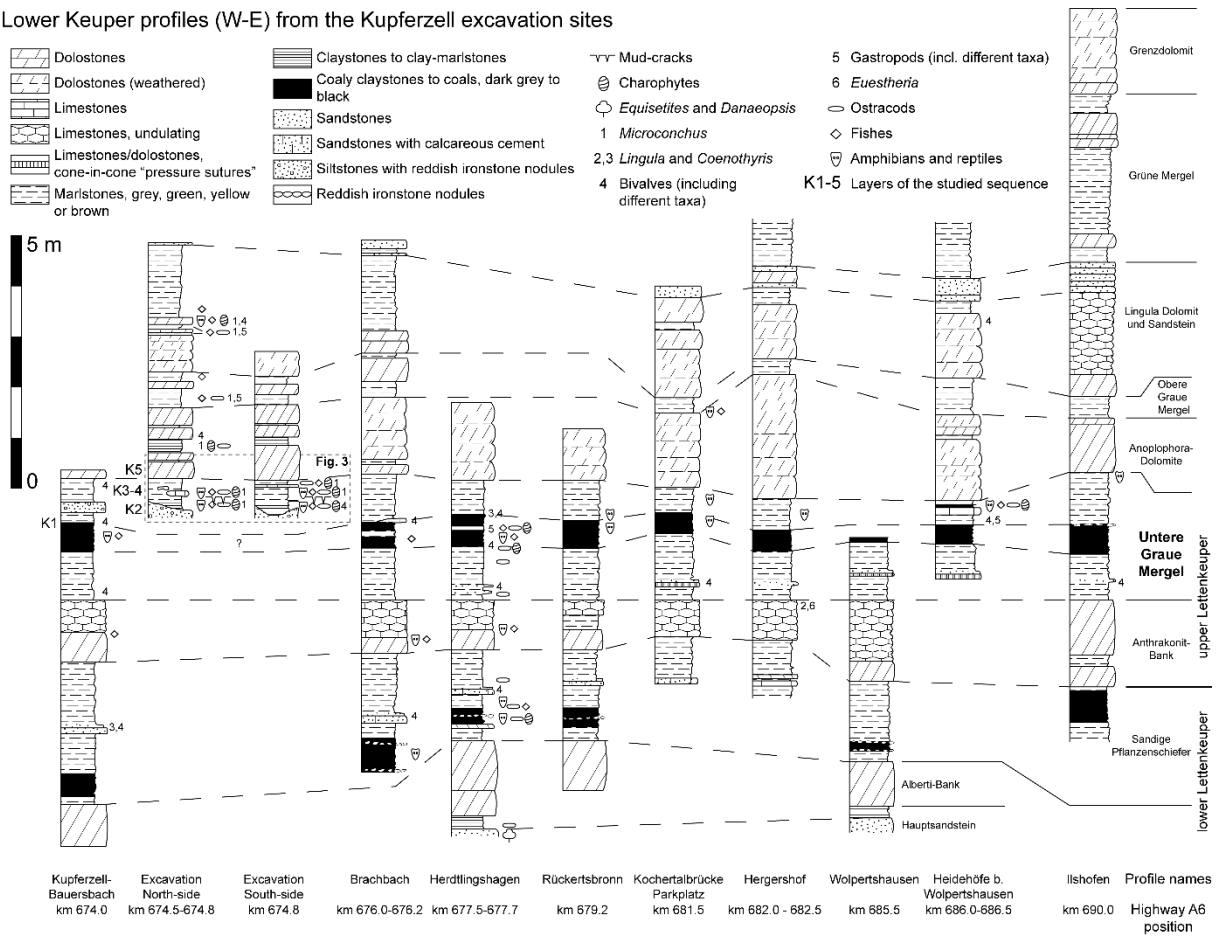
- 1805 Euramerica during the latest Pennsylvanian through Early Permian. In: Fielding,
1806 C.R., Frank, T.D., Isbell, J.L. (Eds.), Resolving the Late Paleozoic Ice Age in Time
1807 and Space. Geological Society of America Special Paper 441, pp. 291-304.
- 1808 Urlichs, M. 1982. Zur Stratigraphie und Fossilführung des Lettenkeupers (Ob. Trias)
1809 bei Schwäbisch Hall (Baden-Württemberg). Jahresberichte und Mitteilungen des
1810 Oberrheinischen Geologischen Vereins 64, 213-224.
- 1811 Voorhies, M.R. 1969. Taphonomy and population dynamics of an early Pliocene
1812 vertebrate fauna, Knox County, Nebraska. Contributions to Geology Special
1813 Paper, University of Wyoming 1, 1-69.
- 1814 Weber, H. 1992. Lettenkeuper-Stratigraphie im Hohenloher Land von F.A. Quenstedt
1815 bis G. Wagner (Trias, Baden-Württemberg). Jahreshefte der Gesellschaft für
1816 Naturkunde in Württemberg 147, 29-58.
- 1817 Wild, R. 1978a. Die Saurier von Kupferzell. Vorläufige Ergebnisse der Fossilgrabung
1818 beim Autobahnbau. Württembergisch Franken 1978, 181-196.
- 1819 Wild, R. 1978b. Massengrab für Saurier. Kosmos 11, 790-797.
- 1820 Wild, R. 1979. Saurier kommen ans Licht. Tierwelt 4, 38-45.
- 1821 Wild, R. 1980. The fossil deposits of Kupferzell, Southwest Germany. Mesozoic
1822 Vertebrate Life 1, 15-18.
- 1823 Winkler, T.C. 1880. Description de quelques restes de poissons fossiles des terrains
1824 triasiques des environs de Wurzburg. Archives du Musée Teyler 5, 109-149.
- 1825 Witzmann, F., Schoch, R.R., Maisch, M.W. 2008. A relict basal tetrapod from Germany:
1826 first evidence of a Triassic chroniosuchian outside Russia. Naturwissenschaften
1827 95, 67-72.
- 1828 Zhao, X., Zheng, D., Xie, G., Jenkyns, H., Guan, C., Fang, Y., He, J., Yuan, X., Xue, N.,
1829 Wang, H., Li, S., Jarzembowski, J., Zhang, H., Wang, B., 2020. Recovery of
1830 lacustrine ecosystems after the end-permian mass extinction. Geology 48, 609-613.
- 1831



1833

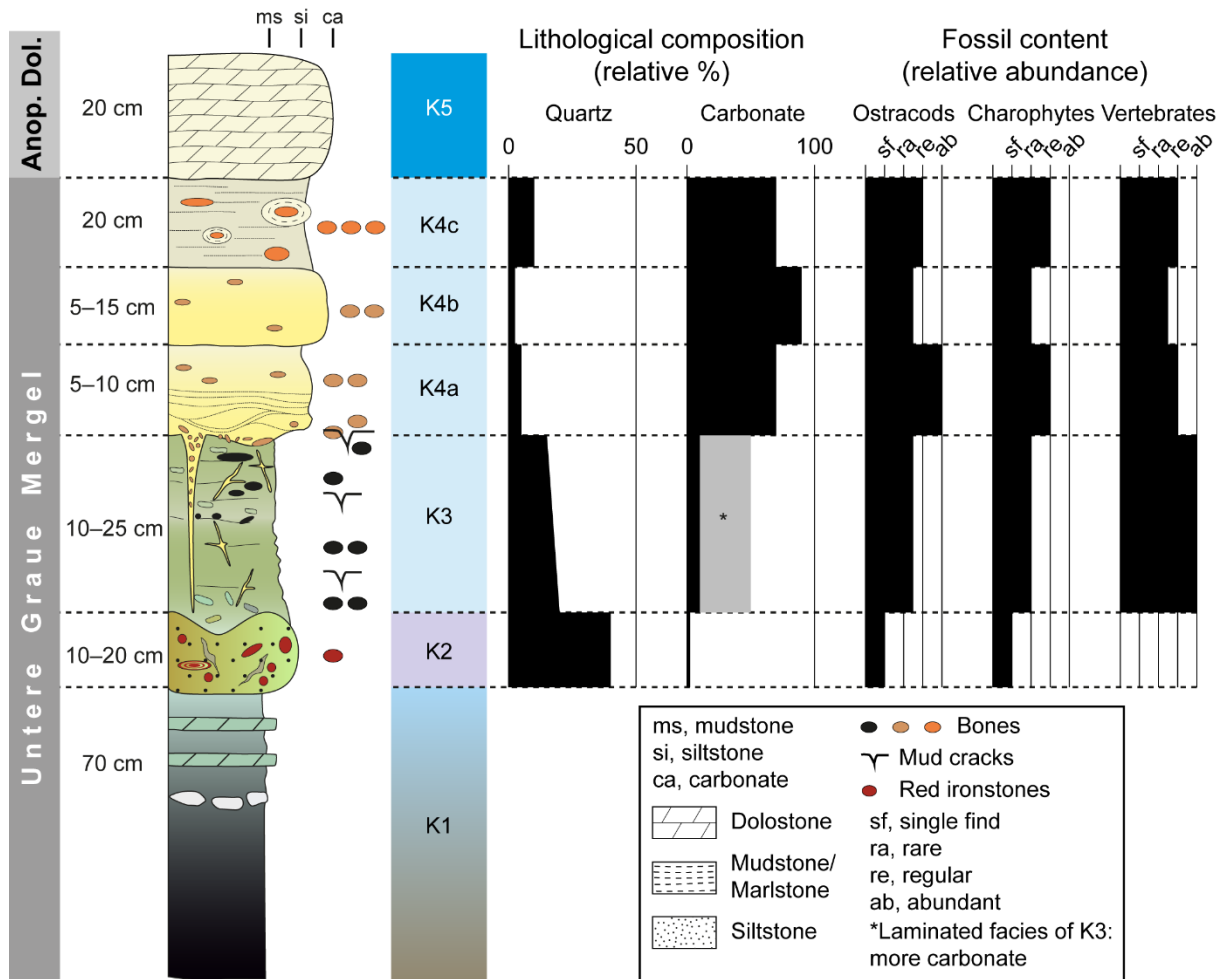
1834 **Figure 1.** Geographical and geological setting. **A**, General stratigraphic section of the
 1835 Lower Keuper and geographic map highlighting the Keuper extension in grey
 1836 (modified from Schoch and Seegis, 2016). **B**, Satellite image (base image from Google
 1837 Earth) showing the different fossil sites (including the two main excavation areas)
 1838 where Lower Keuper sections (see Fig. 2) were logged.

Lower Keuper profiles (W-E) from the Kupferzell excavation sites



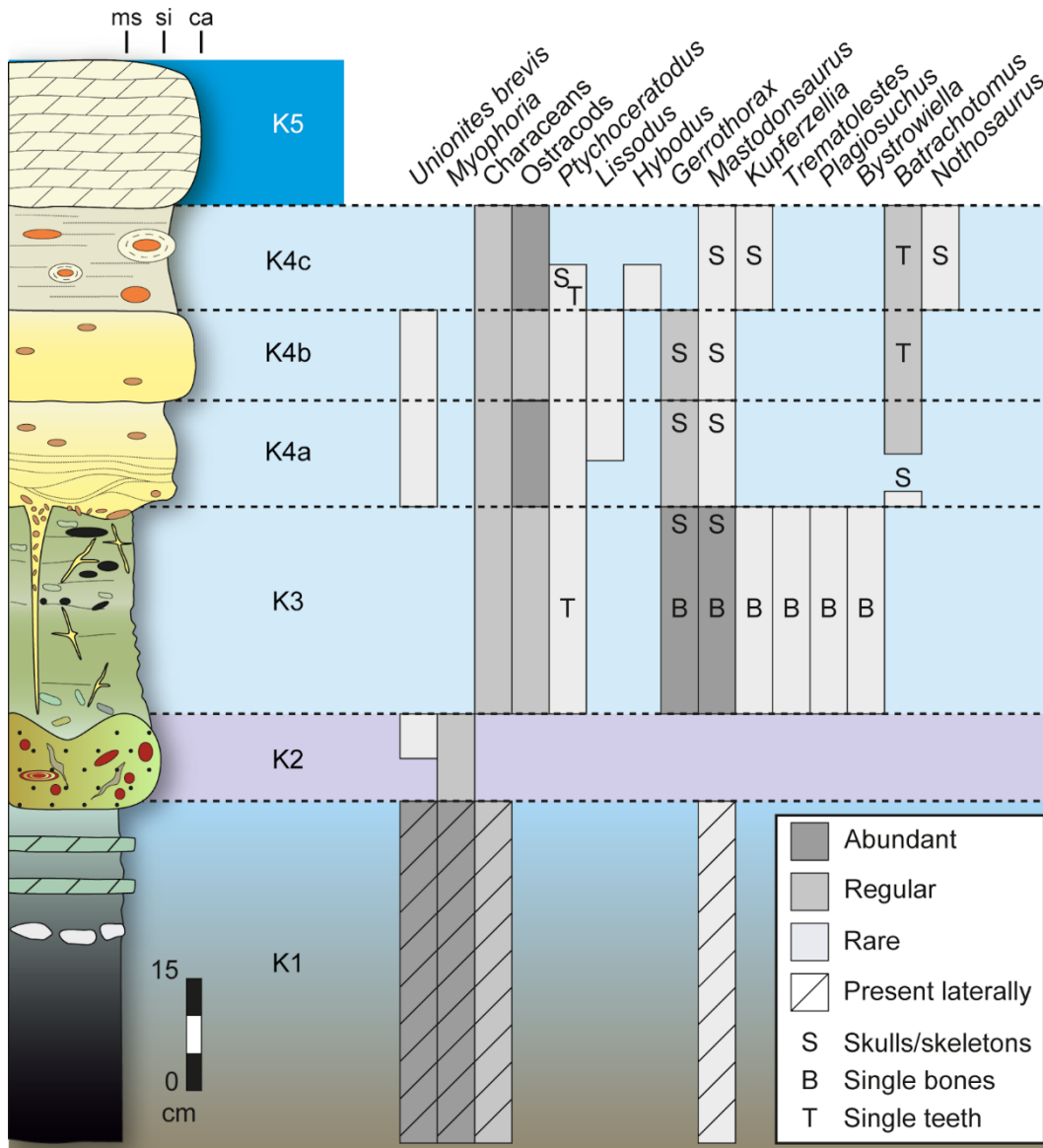
1839

1840 **Figure 2.** Detailed stratigraphic panel of the Lower Keuper at Kupferzell and nearby
 1841 localities along the highway A6. Exact location of each section is shown in Fig. 1B.
 1842 Modified and updated from Urlichs (1982).



1843

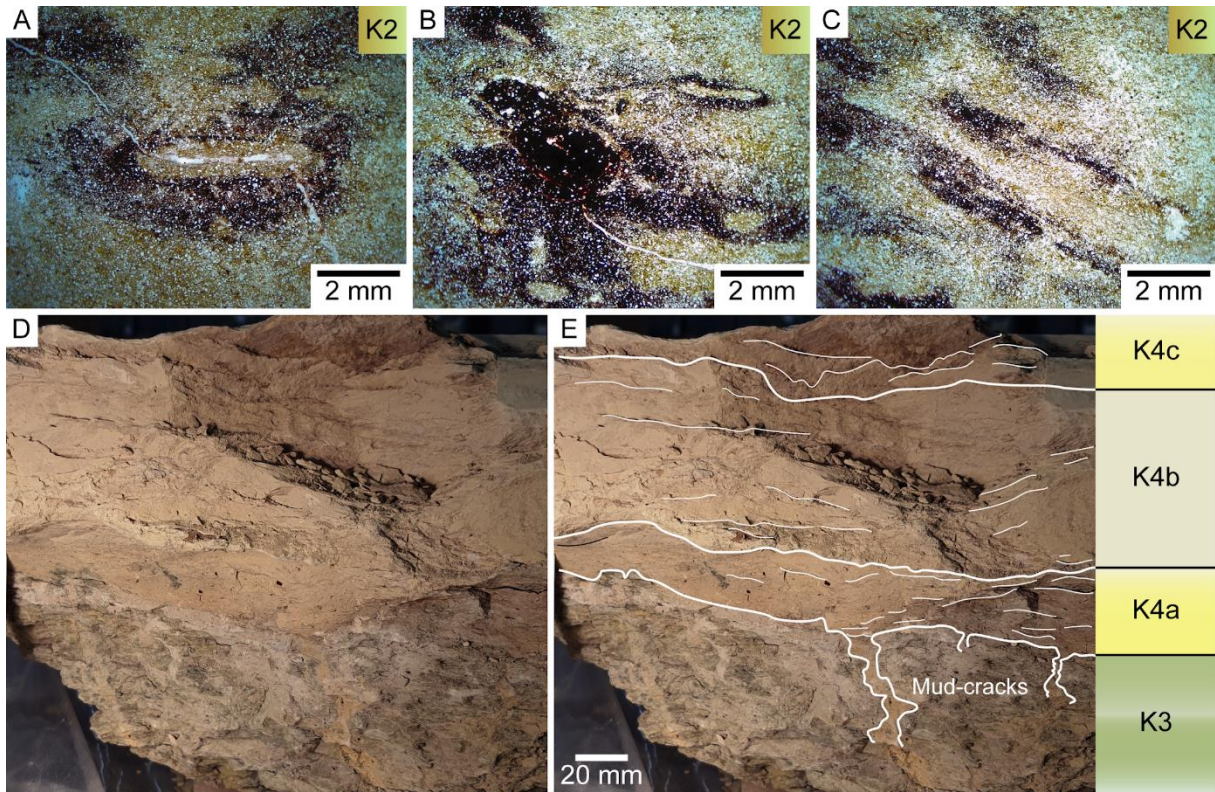
1844 **Figure 3.** Detailed stratigraphic profile of Kupferzell at the main excavation site with
 1845 lithological and sedimentological features, and relative abundance of fossil content.
 1846 Percentages of quartz and carbonate of each unit are based on the petrographic thin
 1847 sections.



1848

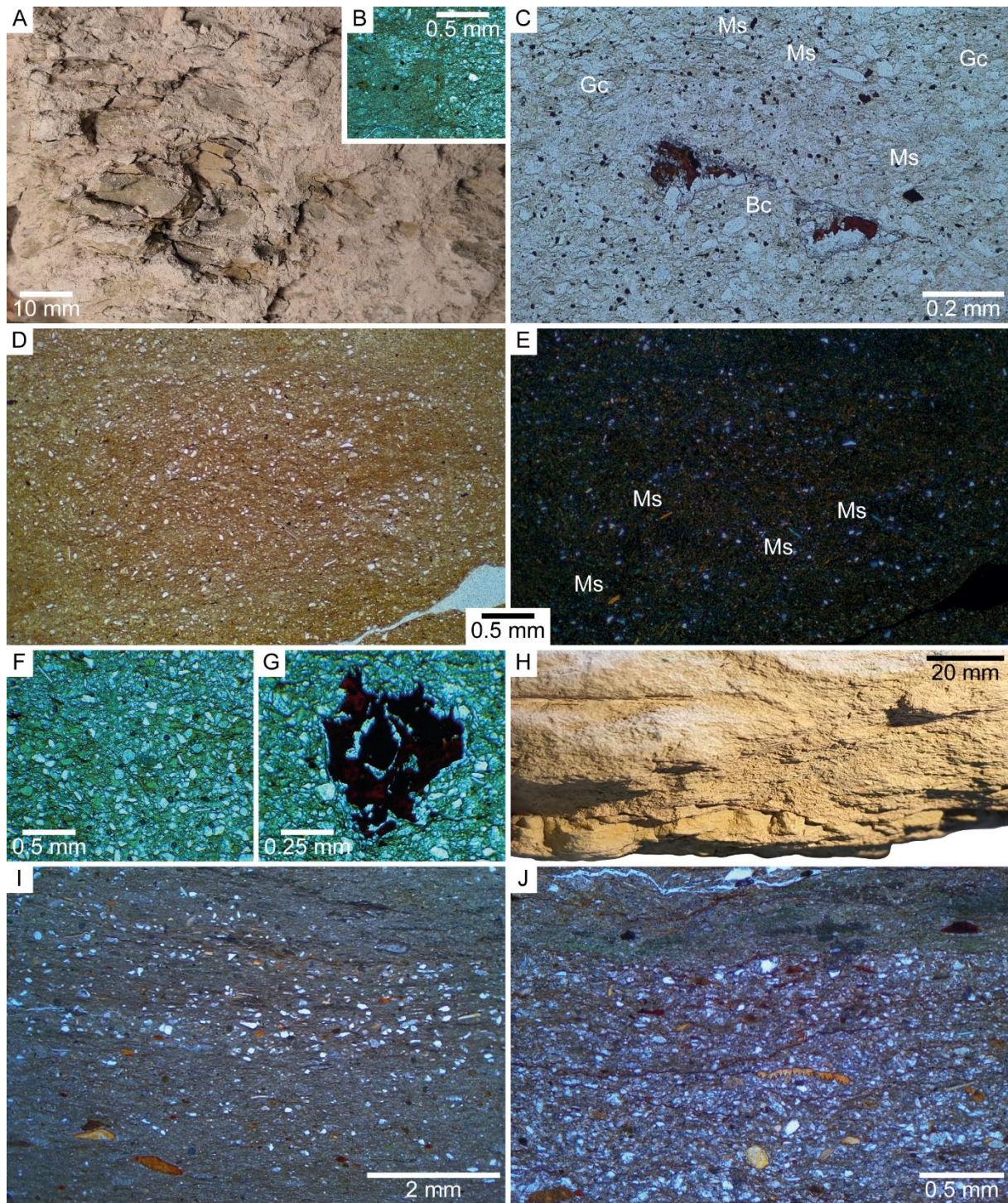
1849 **Figure 4.** Distribution and relative abundance of fossils at the main excavation site in

1850 Kupferzell.



1851

1852 **Figure 5.** Stratigraphy and sedimentological features. **A-C**, Photomicrographs of unit
 1853 K2, siltstones showing a relatively high abundance of quartz grains and the
 1854 characteristic oval-shaped halos making bands (A), with irregular distribution and less
 1855 quartz content (B), and also in oblique orientation with respect to stratification (C). **D-**
 1856 **E**, Hand sample of units K3 (massive facies) and K4 showing the identified layers and
 1857 the characteristic mud-cracks between them.



1858

1859

1860

1861

1862

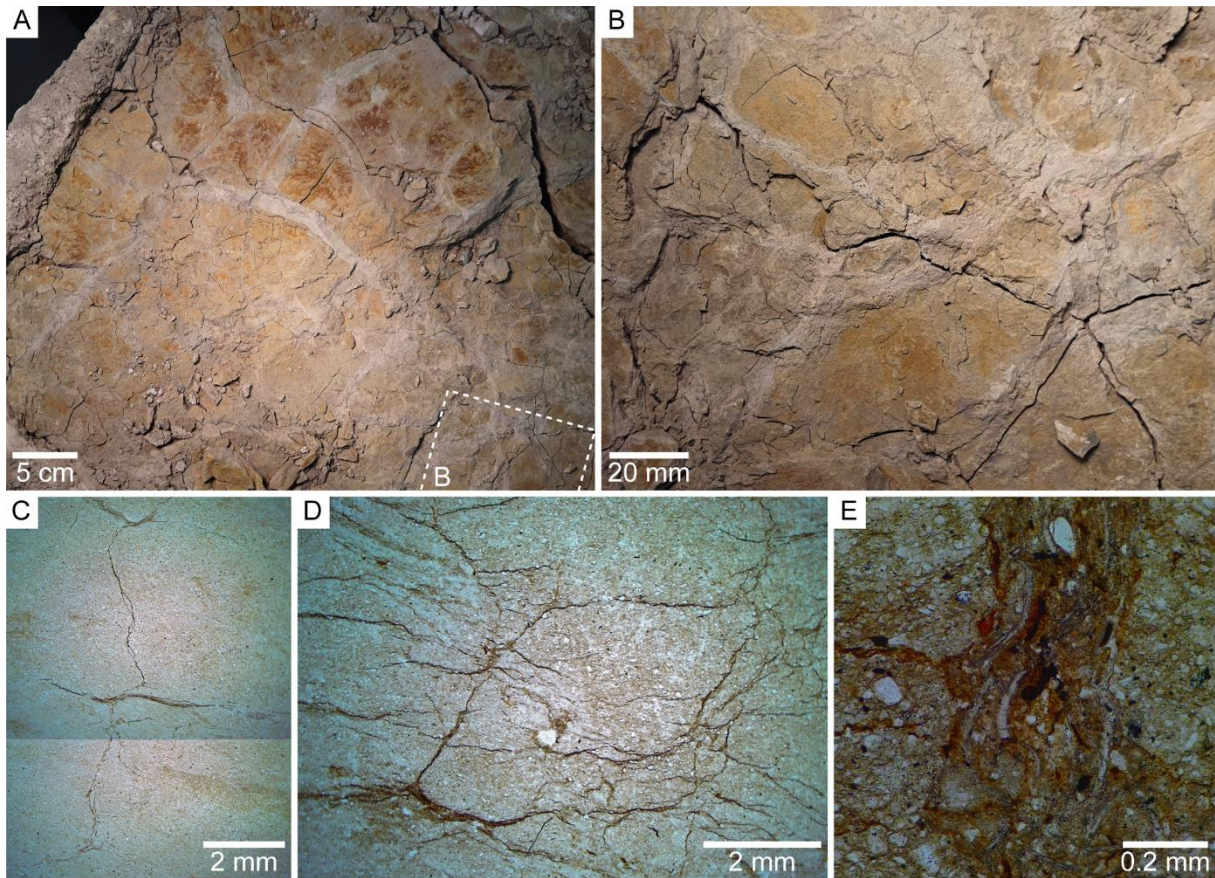
1863

1864

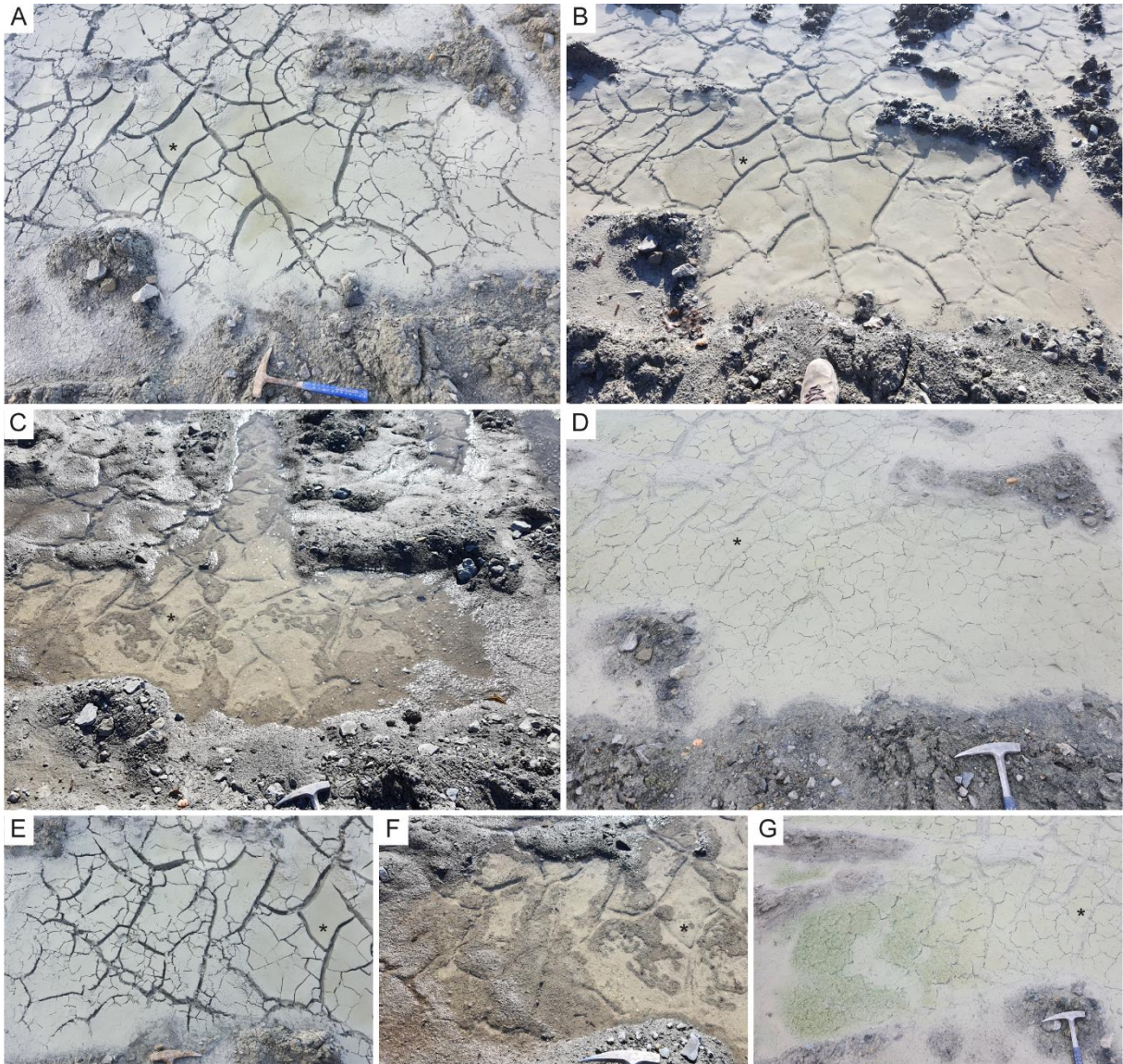
1865

Figure 6. Unit K3. **A-G**, Massive non-carbonate facies (see also Fig. 7); **A**, hand sample of green mudstones with massive aspect and potential aggregations of clayey sediments; **B-G**, photomicrograph showing a relatively high content (~10–20%) of quartz and much less abundant micaceous minerals (~5%) within a clayey matrix with green clasts of chlorite and a few bone fragments; quartz grains are more abundant at the base of the sequence (F), also including red nodules (G) as in K2. **H-J**, Layered/laminated carbonate facies; **H**, hand sample; **I-J**, photomicrographs.

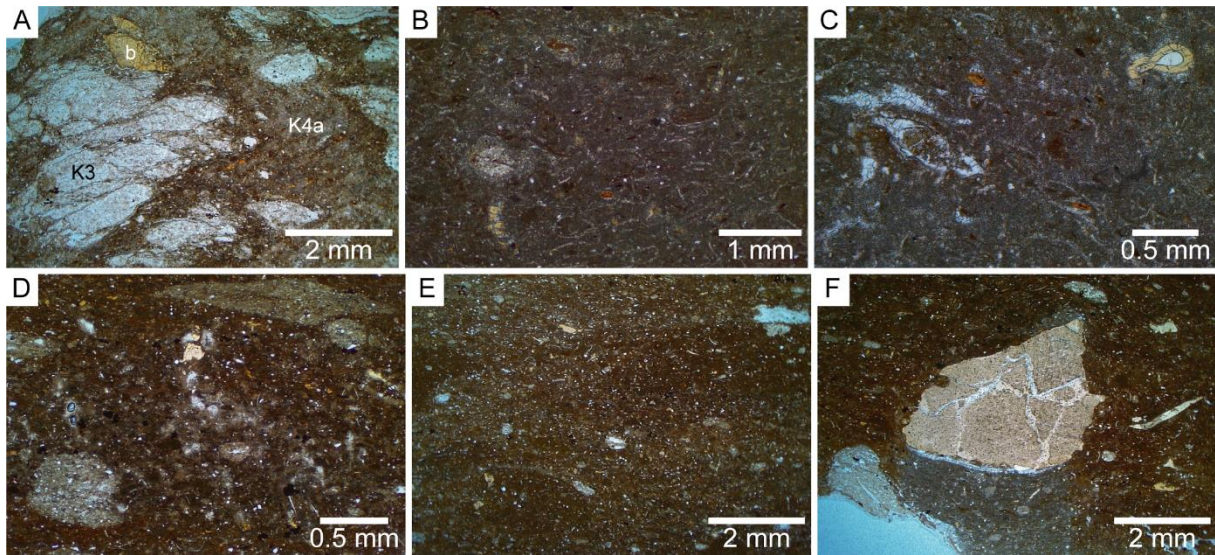
1866 Abbreviations: Bc, bone embedded in calcite; Gc, green clasts (chlorite); Ms, micaceous
1867 minerals.



1868
1869 **Figure 7.** Mud cracks penetrating unit K3. **A-B**, Mud cracks in plain view (bottom
1870 surface of unit K3) showing large and thick mud-cracks in T-junction (A) and smaller
1871 subordinate cracks (B). **C-E**, Photomicrographs of mud cracks (thin dark-brown lines)
1872 from: **C**, the lower part of the unit, where cracks are sparse, mostly vertical lines with
1873 short lateral ramifications; **D**, the upper part showing a denser net of cracks from
1874 vertical to horizontal orientations; **E**, detail of a crack, infilled with ostracod shells and
1875 darker carbonate sediments of layer K4a.

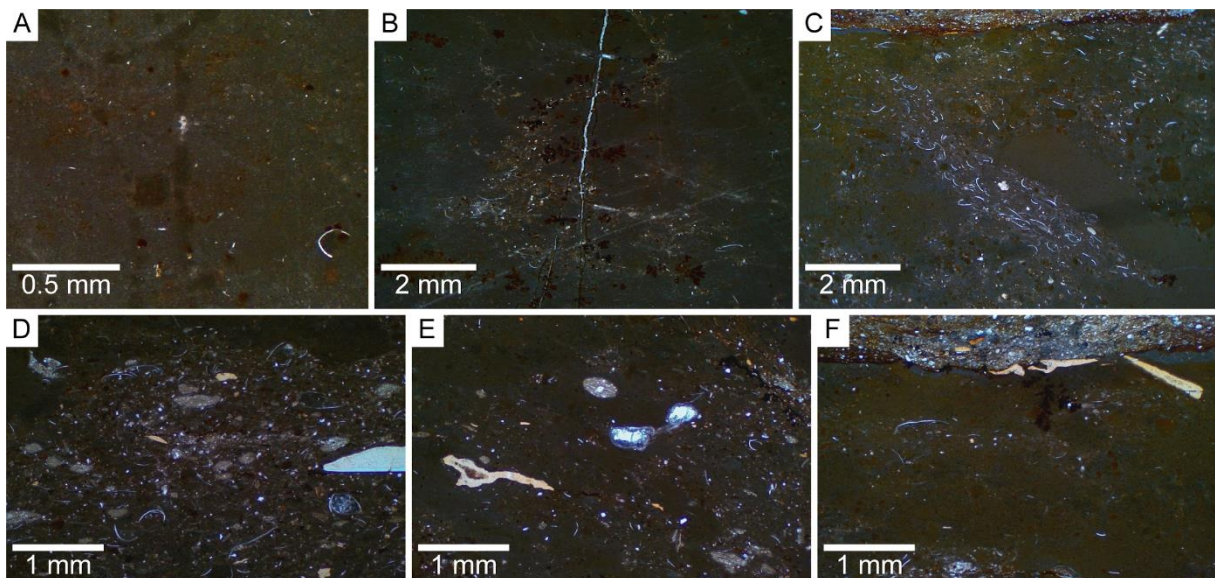


1876
 1877 **Figure 8.** Present-day desiccation mud cracks in T-junction and with smaller
 1878 subordinate cracks developed in a small pond (in both photographs covered by water)
 1879 developed on mud deposits from the Eschenau quarry (sediment originates from the
 1880 Lower Keuper facies mixed with pulverised carbonates from the Muschelkalk facies).
 1881 **A**, Mud cracks recently generated (October 15th, 2021). **B-D**, Progressive covering of
 1882 mud cracks with mud: November 11th, 2021 (B), March 8th, 2022 (C), April 27th, 2022
 1883 (D). **E-G**, Close up of the pond with the fresh cracks (October 15th, 2021; E), their
 1884 infilling (March 8th, 2022; F), and the growing of green algae (April 27th, 2022; G),
 1885 altogether mirroring the environmental evolution between units K3 and K4. Hammer
 1886 in A is 30 cm long. Asterisks (*) indicate equivalent point in all photographs.



1887

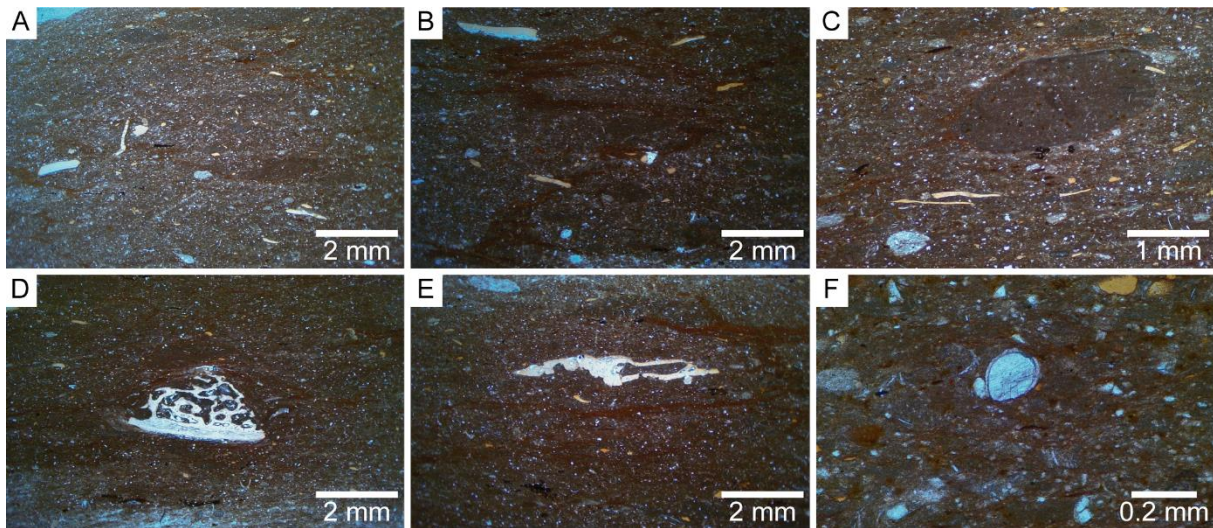
1888 **Figure 9.** Photomicrographs of layer K4a. **A**, Peloids/clasts of layer K3 incorporated
 1889 mostly within the base of the darker layer K4a; bone fragments (b) are also present. **B**,
 1890 General aspect of K4a, being very rich in ostracod shells and less abundant characean
 1891 fragments (e.g., centre-left of the image) within a brown micritic matrix with seldom
 1892 quartz grains. **C**, Bone fragments embedded in sparry calcite. **D-E**, Heterogeneous,
 1893 chaotically organised aspect of the layer, though a rough horizontal and undulated
 1894 lamination is observed. **F**, Large fractured coprolite partially embedded in sparry
 1895 calcite, more concentrated on the bottom surface; below it the layer displays a different
 1896 aspect, possibly due to (re-) precipitation of carbonate diagenetic fluids.



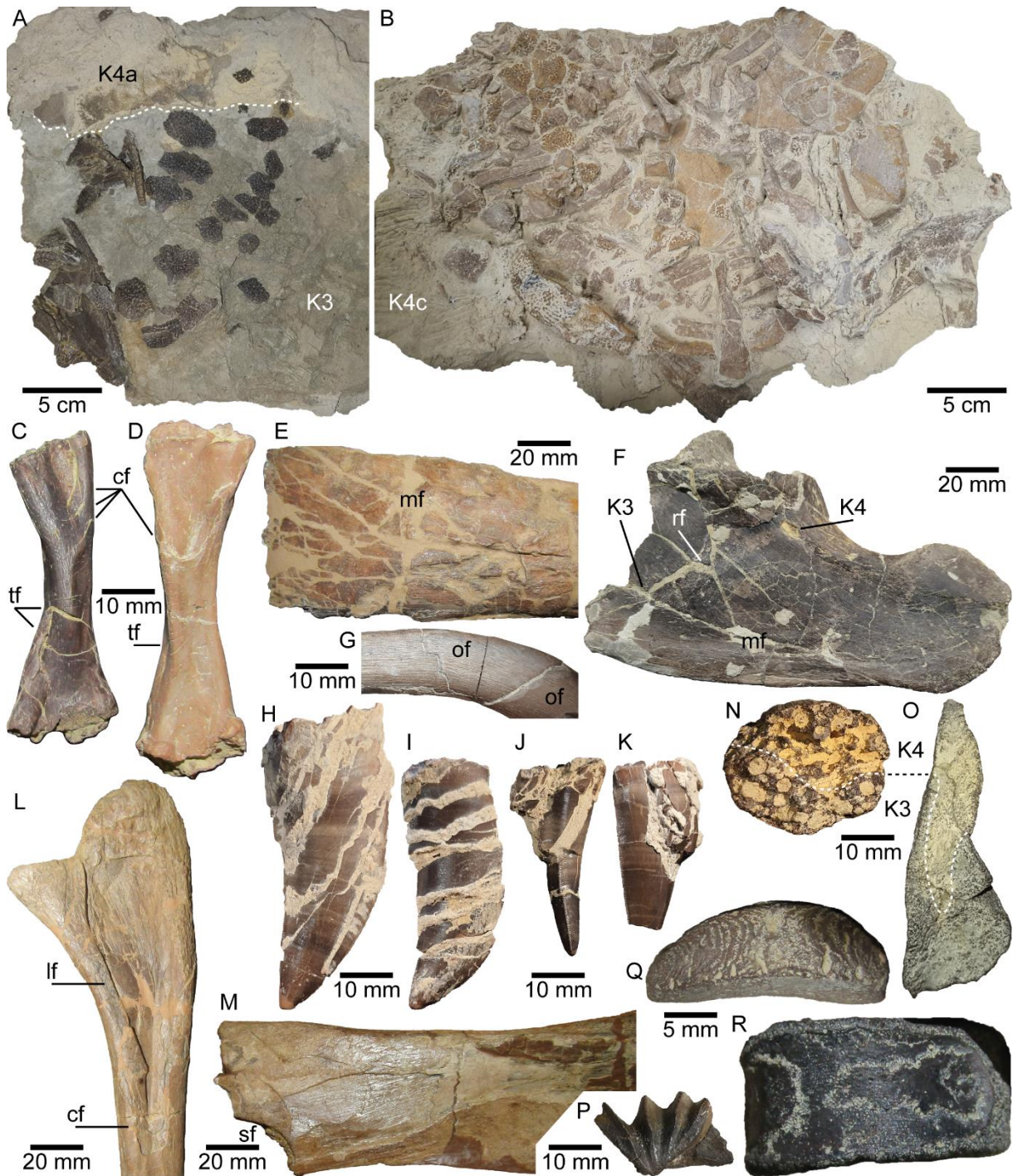
1897

1898 **Figure 10.** Photomicrographs of layer K4b. **A**, Typical aspect of the layer (wackestone),
 1899 being a massive micritic brown carbonate with rounded darker stains, possibly
 1900 diagenetic peloids, and with seldom ostracods shells, bioclasts and very sporadic

1901 quartz grains. **B-C**, Potential burrows infilled with a coarser (lighter coloured) matrix
1902 with abundant ostracods and subordinate quartz grains. **D-E**, Chaotically organised
1903 portions containing more abundant bioclasts, mainly including ostracods, characeans
1904 and bones. **F**, Boundary with layer K4c (see also top part of C), which is sharp and
1905 undulated, indicating potential erosion.



1906 **Figure 11.** Photomicrographs of layer K4c. **A-B**, Typical aspect, with irregularly
1907 distributed horizontal seams, abundant ostracod shells and subordinate bone
1908 fragments (sometimes oblique to stratification) and quartz grains; note similarities
1909 with layer K4a. **C**, Relatively large oval-shaped peloid, possibly being a reworked clast
1910 of the same layer. **D-E**, Large well preserved bone fragments partially embedded in
1911 sparry calcite. **F**, Detail of the layer with a well preserved, but slightly eroded
1912 (abraded) characean oogonia.
1913

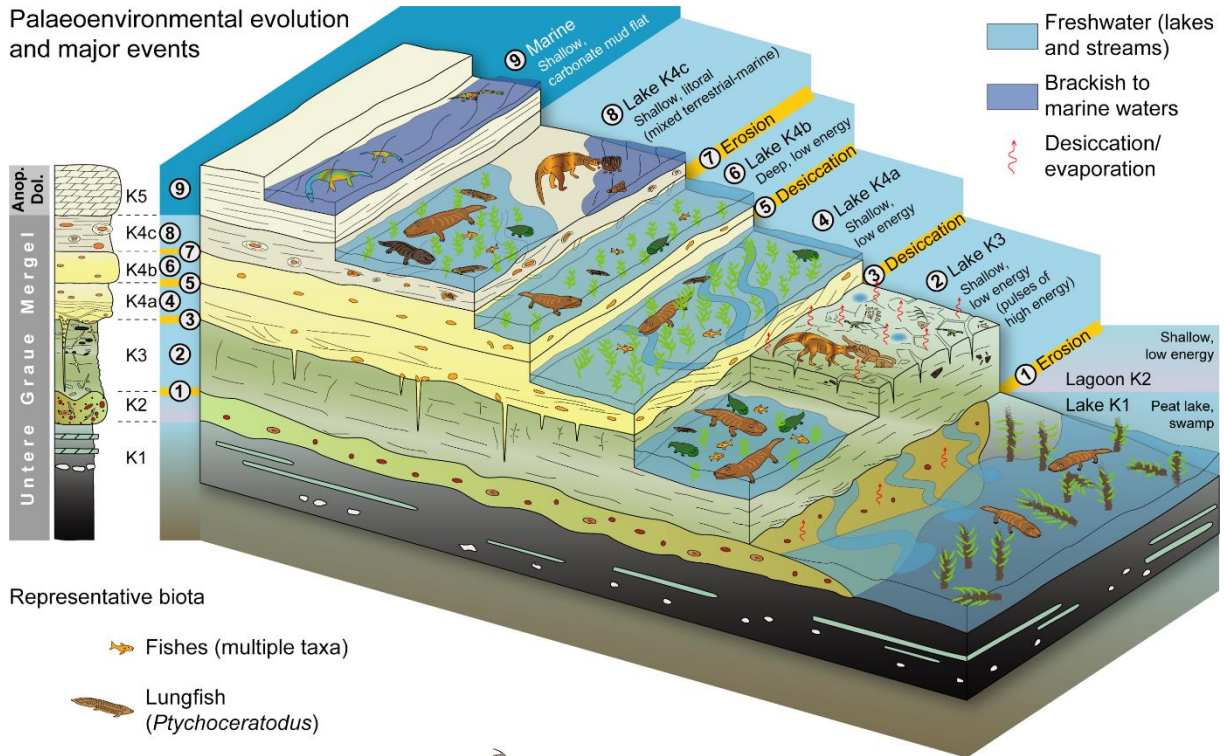


1914

1915 **Figure 12.** Taphonomic features of tetrapod remains from Kupferzell. **A-B**, Skeletons
 1916 of *Gerrothorax* showing different preservations linked to the sedimentary unit; **A**,
 1917 partial, disarticulated skeleton with bones chaotically oriented on top of unit K3. **B**,
 1918 Fairly complete, disarticulated (but with elements approximately in place) skeleton
 1919 covered with a carbonate crust within layer K4c. **C-D**, Femora of *Gerrothorax* (SMNS
 1920 81450 (C), 81454 (D)) showing different coloration according to the unit (C is from K3
 1921 and D is from K4) as well as semi-circular (cf) and transverse (tf) fractures. **E**, Right
 1922 hemimandible of *Batrachotomus* (SMNS 52970) showing a mosaic pattern of fractures

1923 (mf). **F**, Mandible fragment of *Mastodonsaurus* with sedimentary matrix of both units
1924 K3 and K4, as well as radial fractures (rf) and a mosaic pattern of fractures (mf) types.
1925 **G**, Dorsal rib of *Nothosaurus* (SMNS 80266) with spiral to oblique fractures (of)
1926 including right angle offsets (fracture on the left). **H-K**, Teeth of *Batrachotomus*
1927 showing multiple parallel fractures infilled with calcitic sediment and completely
1928 dividing the teeth in neat breaks (H, I), as well as fractures infilled with sediment and
1929 teeth fragments displaced chaotically (J, K). **L**, Proximal end of a *Batrachotomus* right
1930 ulna (SMNS 80275) with longitudinal (lf) and semi-circular (cf) fractures. **M**, Distal end
1931 of a *Batrachotomus* right pubis (SMNS 52970) with a spiral fracture (sf). **N-O**, Tusk
1932 (SMNS 83276 (N)) and left humerus (SMNS 81171 (O)) of *Mastodonsaurus* with
1933 sedimentary matrix of both units K3 and K4; note also the round holes in the base of
1934 the tusk, possibly due to chemical dissolution. **P**, Dipnoan mandible tooth (SMNS
1935 56866) with the enameloid abraded. **Q-R**, Small-sized vertebral centra of
1936 *Mastodonsaurus* (SMNS 84094 (Q), 84098 (R)) with chemically abraded surfaces.

Palaeoenvironmental evolution and major events



Representative biota

- Fishes (multiple taxa)
- Lungfish (*Ptychoceratodus*)
- Plagiosaurs (*Gerrothorax*)
- Medium to large capitosaurs (*Kupferzellia*)
- Large capitosaurs (*Mastodonsaurus*)
- Tetrapod carcasses (usually scavenged)
- Small-sized archosauriformes
- Large archosaurs (*Batrachotomus*)
- Tanystropheus*
- Neusticosaurus*
- Nothosaurus*
- Characeans
- Large tree-like plants

1937

1938

1939

1940

Figure 13. Reconstruction of the palaeoenvironmental evolution in Kupferzell. The main events are indicated and the most representative taxa and sedimentary structures are depicted.